Syracuse University

SURFACE

2013

Studies Towards Identifying the Active Site Structure of Human Ghrelin O-Acyltransferase (HGOAT)

Rosemary Loftus

ABSTRACT

Ghrelin is a peptide hormone involved in appetite stimulation, regulation of insulin signaling, and other physiological processes. Ghrelin requires acylation of the hydroxyl group of a specific serine residue with an octanoyl group to bind its receptor and activate signaling. This modification is catalyzed by ghrelin *O*-acyltransferase (GOAT). Ghrelin is the only known substrate of GOAT, making GOAT inhibition a promising avenue for treatment of obesity and type II diabetes. Understanding the interactions between ghrelin and GOAT responsible for binding and catalysis will aid in developing specific GOAT inhibitors.

To identify the nature and location of the ghrelin binding site and active site within human GOAT (hGOAT), we have generated a series of hGOAT mutants. The ghrelin acylation activity of these mutants will be tested to ascertain which regions of hGOAT are essential for function. To develop a profile of the binding site for the acyl-coenzyme A cosubstrate of hGOAT, acyl CoA donors with varying acyl lengths were tested for ghrelin acylation activity with hGOAT. Identifying the hGOAT active site and substrate binding site will aid in hGOAT characterization and provide information for development of hGOAT inhibitors.

SYRACUSE UNIVERSITY

STUDIES TOWARDS IDENTIFYING THE ACTIVE SITE STRUCTURE OF

HUMAN GHRELIN O-ACYLTRANSFERASE (HGOAT)

A THESIS SUBMITTED TO

THE FACULTY OF THE DIVISION OF PHYSICAL SCIENCES

IN CANDIDACY FOR THE DEGREE OF

MASTERS OF SCIENCE

DEPARTMENT OF CHEMISTRY

BY

ROSEMARY JEAN LOFTUS

SYRACUSE, NY

JUNE 2013

TABLE OF CONTENTS

LIST OF FIGURES

LIST OF TABLES

ABBREVIATIONS

GHS-R	Growth-hormone secretagogue receptor
GH	Growth hormone
GOAT	Ghrelin O-acyltransferase
hGOAT	Human ghrelin O-acyltransferase
MBOAT	Membrane-bound O-acyltransferase
TMHMM	TransMembrane by Hidden Markov Model
DNTP	Deoxyribonucleotide triphosphate
PCR	Polymerase chain reaction
LB	Luria-Bertani
P1 virus	Passage 1 virus
P2 virus	Passage 2 virus
MOI (pfu/cell)	Multiplicity of Infection (plaque forming unit/cell)
HPLC	High Performance Liquid Chromatography
MBP	Maltose binding protein
GST	Glutathione S-transferase
IPTG	isopropyl-β-D-thiogalactopyranoside
T7RNAP	T7 RNA polymerase

INTRODUCTION

Ghrelin is a 28 amino-acid peptide hormone that was discovered in 1999 by Kojima and coworkers in the search for the ligand for the growth-hormone secretagogue receptor (GHS-R1a), a G-protein coupled receptor.[1] Ghrelin binds and activates GHS-R1a, leading to the release of growth hormone (GH) from the pituitary gland.[1] The mechanism for ghrelin-stimulated release of GH proceeds through a series of steps, beginning with ghrelin binding to GHS-R1a to activate phospholipase C. This activation generates inositol triphosphate (IP$_3$) and diacylglycerol, which leads to increased cellular Ca^{2+} concentrations that causes the release of GH.[1, 2]

Upon the discovery of ghrelin, Kojima and coworkers analyzed both naturally isolated rat ghrelin and a chemically synthesized ghrelin by reverse-phase HPLC.[1] The natural ghrelin exhibited a 10-minute delay in retention time relative to the synthetic ghrelin, suggesting that ghrelin is modified by a hydrophobic moiety. Using mass spectroscopy, it was found that an eight carbon fatty acid (octanoate) acylates the third serine (Ser3) residue of ghrelin, a previously unknown peptide modification. Subsequent studies have shown that the Ser3 of ghrelin must be acylated (unacylated ghrelin is referred to as des-acyl ghrelin) to exert its endocrine activity through GHS-R binding.[1, 3, 4, 5]

Ghrelin is secreted primarily from the stomach and other organs in the gastrointestinal tract.[6, 7, 8] Ghrelin is known to stimulate hunger, as indicated by the ability of injected ghrelin to stimulate eating in rodents.[8, 9, 10, 11] The role of ghrelin in stimulating appetite is consistent with the increased ghrelin concentrations commonly observed in human plasma before mealtimes.[12]

Patients suffering from anorexia nervosa also exhibit increased ghrelin concentrations.[8, 13, 14] The role of ghrelin in obesity is complex, as decreased plasma concentrations of ghrelin are often observed in obese patients.[10, 15] This may suggest that ghrelin signaling is disrupted in these patients, possibly leading to aberrant coupling between ghrelin levels and appetite.[16, 17, 18] However, patients suffering from the genetic disease Prader-Willi syndrome exhibit elevated ghrelin levels.[19] This disease is characterized by a number of symptoms including severe obesity and constant hunger, suggesting a potential link between elevated ghrelin levels and insatiable appetite.[1, 19, 20]

Ghrelin is also potentially linked to insulin signaling and diabetes. Although produced predominately in the stomach, both ghrelin and its GHS-R1a receptor have been identified in pancreatic islets that are responsible for secreting insulin.[4, 21, 22] Studies have shown that administration of ghrelin inhibits insulin secretion in rodents, and reduces insulin sensitivity in humans, thereby blocking glucose-stimulated insulin secretion.[23, 24, 25] However, upon injection of des-acyl (non-acylated) ghrelin in rodent islet β-cells, the same inhibitory effect on insulin secretion is not observed,[26] suggesting that perhaps glucose homeostasis can be regulated with varying ratios of ghrelin to des-acyl ghrelin.[27, 28] A therapeutic option for type II diabetic patients could be available if the ghrelin to des-acyl ghrelin ratio could be regulated, thereby controlling for insulin resistance and sensitivity.

Like many secreted proteins, ghrelin undergoes a number of processing steps after translation by the ribosome.[29, 30] One of these maturation steps involving serine octanoylation appears to be unique to ghrelin. Ghrelin is initially translated as a 117-amino acid precursor protein, preproghrelin, which is then trafficked to the endoplasmic reticulum (ER). In the first posttranslational processing step, the N-terminal 23 amino acid secretory signal peptide sequence

of preproghrelin is excised by a signal peptidase to yield the 94 amino acid proghrelin. Proghrelin is proposed to serve as the substrate for ghrelin *O*-acyltransferase (GOAT), which catalyzes octanoylation of the serine 3 residue. After acylation by GOAT and trafficking to the Golgi, prohormone convertase 1/3 (PC 1/3) cleaves acylated proghrelin after arginine 28 to produce mature ghrelin. Following maturation, both acylated and unacylated ghrelin are packaged into vesicles and released into the bloodstream (Figure 1).[30, 31, 32]
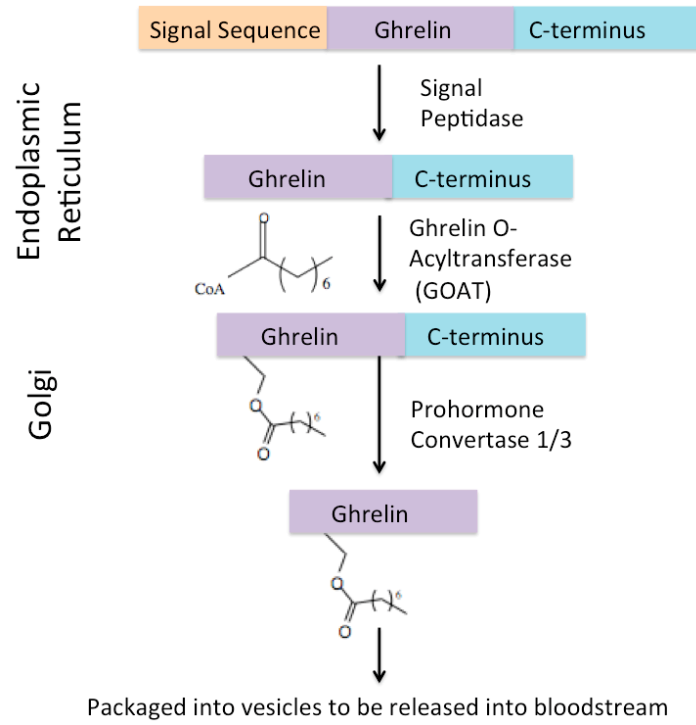
Figure 1. Processing of prepro-ghrelin to mature ghrelin peptide.

In 2008, two laboratories simultaneously identified the 49 kDa enzyme responsible for catalyzing the octanoylation of ghrelin, naming it ghrelin *O*-acyltransferase (GOAT, Figure 2).[33, 34] GOAT is the fourth member of the membrane-bound *O*-acyltransferase (MBOAT) family composed of integral membrane enzymes that catalyze acylation of a range of small molecule and protein substrates, among which include hedgehog acyltransferase (Hhat) which acylates the secreted protein sonic hedgehog, and porcupine (Porc) which acylates Wnt.[35, 36, 37, 38, 39] Yang and coworkers identified GOAT by transfecting a variety of MBOAT family acyltransferases into the INS-1 cell line, which contains a mixture and proghrelin and mature ghrelin, and found that octanoylated ghrelin was produced when GOAT was transfected.[33] In this study, acylation of Ser3 of ghrelin by octanoate was verified using labeling with radioactive octanoic acid. Yang and coworkers also used site-directed mutagenesis to mutate two highly conserved residues across the MBOAT family to alanine (Asn307 and His338) and found that mutation of these residues led to a loss of GOAT-catalyzed ghrelin acylation. This loss of activity suggests that these conserved residues may be important for catalysis.[33] Gutierrez and coworkers employed a different approach to identify GOAT, using gene-silencing of a number of known acyltransferase sequences to screen for GOAT.[34] In this study, modification of Ser3 with the octanoate group was verified using mass spectrometry fragmentation analysis.[34] When the gene for GOAT was silenced, only desacyl ghrelin was detected providing a functional linkage between GOAT expression and ghrelin octanoylation.
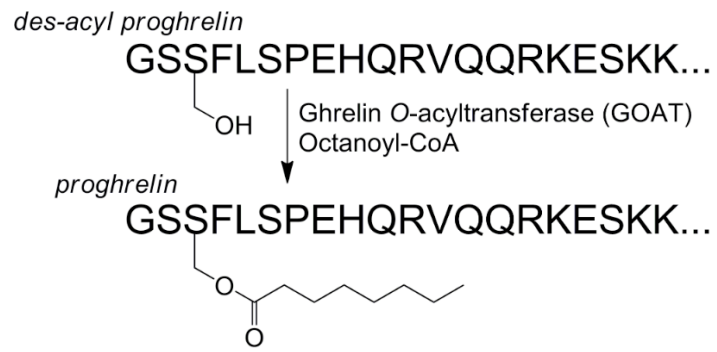
Figure 2. hGOAT-catalyzed octanoylation of proghrelin.

In a subsequent study, Yang and coworkers developed an *in vitro* GOAT activity assay using membrane fraction isolated from insect cells infected with recombinant baculovirus encoding mouse GOAT.[40] Using recombinantly expressed proghrelin as a substrate, Yang sought to identify the amino acids surrounding Ser3 of proghrelin involved in substrate recognition by mouse GOAT using alanine scanning mutagenesis. This study indicated that the first five amino acids at the N-terminus of proghrelin (GSSFL), in the context of a C-terminally amidated peptide, were sufficient to serve as both a substrate of GOAT and an inhibitor of GOAT-catalyzed octanoylation of proghrelin. Pentapeptides with an Ala mutation in place of Ser3 also serve as GOAT inhibitors without being octanoylated, suggesting that Ser3 is required for activity but not substrate binding.[40] Yang also found that octanoylated peptides, the product of GOAT-catalyzed peptide acylation, serve as more effective inhibitors than the non-acylated peptides. This observation of product inhibition raises the possibility of feedback inhibition of GOAT, which was tested by substituting the octanoyl (C8) group on the acylated peptide with longer acyl chains such as myristoyl (14 carbons) and palmitoyl (16 carbons). Peptides bearing these longer acyl modifications proved to be less effective GOAT inhibitors, suggesting that the acyl chain binding site of GOAT selects for medium length acyl groups such as octanoate, a finding supported by other studies.[41] Yang and coworkers also found that replacement of the ester in octanoyl ghrelin by an amide, through substitution of serine 3 with (S)-2,3-diaminopropionic acid (Dap), led to a significant increase in inhibitor binding.[40] While this substitution leads to a much more stable bond between the ghrelin peptide and the octanoyl group due to the ester-amide substitution, the underlying cause for the observed increase in inhibitor affinity remains undefined.

In addition to the work by Yang and coworkers using short peptides[40] several other routes have been explored to identify potential GOAT inhibitors. The Cole laboratory designed a "bisubstrate" inhibitor that is capable of crossing mammalian cell membranes.[42] This peptide-based inhibitor (GO-CoA-Tat) links the first 10 amino acids of ghrelin to octanoyl CoA using an amide bridge, with a polybasic Tat sequence attached to the peptide C-terminus to enhance cell penetration. The GO-CoA-Tat inhibitor reduced weight gain and increased glucose tolerance in mice, and also altered feeding behavior in hamsters.[42, 43] Janda and coworkers have also explored the potential for small-molecule libraries to yield efficient GOAT inhibitors.[44, 45] Although these inhibitor studies have yielded some promising results, defining the active site of GOAT and the interactions used by GOAT to bind and recognize ghrelin is critical to developing effective and potent GOAT inhibitors as potential therapeutics.

Development of a model of how recombinant human GOAT (hGOAT) binds and recognizes ghrelin requires identifying the interactions involved in forming the hGOAT-ghrelin complex. Using a novel fluorescent peptide substrate that mimics the N-terminal sequence of ghrelin, Darling and coworkers in the Hougland lab have employed structure-activity studies to define the interactions between hGOAT and ghrelin involved in substrate binding and catalysis.[46] By mutating amino acids of the ghrelin peptide mimic (GSSFLC$_{AcDan}$) and substituting functional groups, they were able to identify multiple interaction points between the hGOAT active site and the ghrelin substrate. For example, their work suggests that recognition of the Ser2 residue of ghrelin is based on both steric size of the amino acid at this position as well as the serine hydroxyl side chain. They also found that the N-terminal amine and lack of side chain at the N-terminal glycine residue (Gly1) is critical to hGOAT recognition of ghrelin, as mutating the Gly1 residue or acetylating the N-terminal amine eliminated activity with hGOAT.[46] This

8

work identifies specific functional groups on the ghrelin substrate that interact with the hGOAT active site, but does not provide information on the groups on the enzyme involved in these contacts.

To complement the studies of hGOAT selectivity using modified peptide substrates, my research has focused on determining residues and regions of hGOAT involved in substrate recognition and catalysis in order to enhance understanding of the hGOAT active site structure. Using mutagenesis and enzyme truncation, I have worked to define the contribution of specific residues within hGOAT to enzyme function. To investigate the acyl donor binding pocket of hGOAT, I have screened acyl CoA cosubstrates with varying acyl chain lengths for ghrelin acylation activity with hGOAT. Defining the active site structure and catalytic mechanism of hGOAT will contribute to the development of potent hGOAT inhibitors for evaluation as treatments for obesity, diabetes, Prader Willi Syndrome, and other conditions.

CHAPTER TWO

CONSTRUCTION OF GHRELIN O-ACYLTRANSFERASE VARIANTS

Introduction

Ghrelin *O*-acyltransferase (GOAT) catalyzes an essential step in the maturation of the peptide hormone ghrelin, which is centrally involved in hunger signaling.[33] Development of targeted GOAT inhibitors is proposed to be a route to novel therapeutics for treating obesity, diabetes, and a range of other conditions.[3, 8, 40, 42, 43, 45] The design and optimization of GOAT inhibitors will be aided by a molecular-level understanding of the active site of GOAT. As GOAT is an integral membrane protein, structural studies face significant experimental challenges due to the intransigence of membrane proteins to protein crystallographic study. In light of this challenge, we have pursued biochemical and functional studies to localize the residues and regions that form the active site within the human isoform of GOAT (hGOAT).

While the extremely hydrophobic character and structural complexity of hGOAT as an integral membrane protein renders identification of the active site difficult, we can use computational methods and mechanistic reasoning to rationally search for this region. The first example of this approach deals with identifying the domains within hGOAT required for enzyme function. The transmembrane topology of the human isoform of GOAT (hGOAT) has not been experimentally investigated,[33] but computational algorithms such as TMHMM (TransMembrane by Hidden Markov Model) can provide a prediction of hGOAT domain structure (Figure 3).[47] This algorithm predicts that hGOAT contains seven transmembrane helices connected by six soluble "loops" that are not embedded in the membrane. These loop regions are good candidates

for the location of the hGOAT active site. The location of Asn307 and His338, two conserved

residues that have been shown to be important for GOAT activity, within the Loop D region

provides further evidence that the hGOAT active site may lie within one or more of the predicted

loop regions.[33] Using both truncations from the protein N-terminus and expression of the

predicted loop domains, we will assess which domains within hGOAT are required for enzyme

activity.
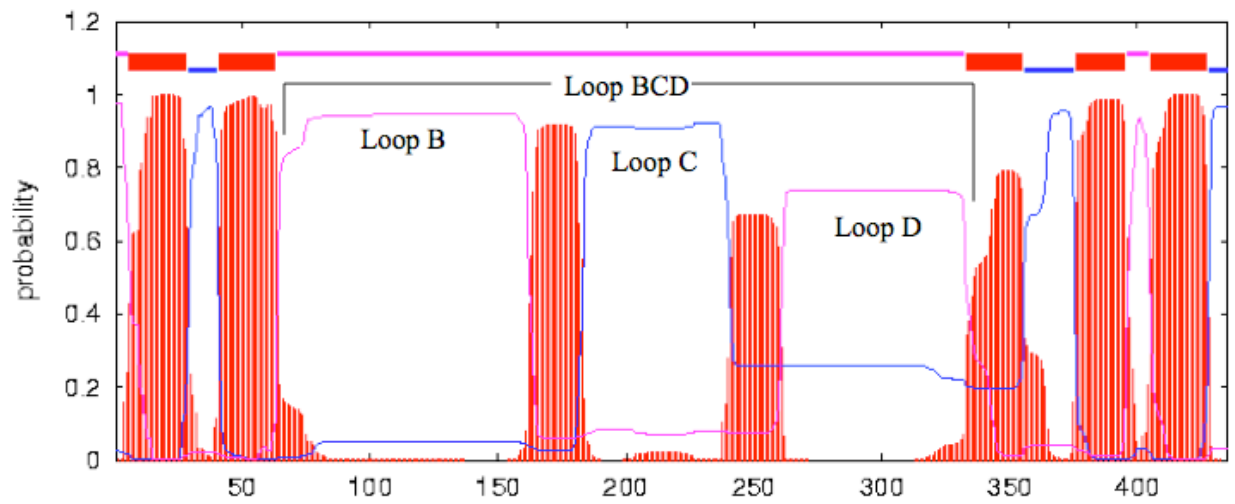
Figure 3. TMHMM prediction for transmembrane helices and loop domains within hGOAT. The red shows the predicted transmembrane residues, the blue shows the residues predicted to lie inside the membrane, and the pink shows the residues predicted to lie outside the membrane.[47]

In addition to assessing the functional requirement for individual hGOAT domains, site-directed mutagenesis was also performed to investigate the potential roles of specific amino acid residues within hGOAT for catalytic activity and/or hGOAT structure. For this analysis, only residues located in the loop regions of hGOAT were taken into consideration, as these residues would be more accessible to bind the substrate during catalysis. The individual sites for mutagenesis were chosen based on amino acid conservation, potential to serve as a ligand for a catalytic metal ion, and potential to act as part of charge-relay system for activating the serine 3 of ghrelin as a nucleophile. The hGOAT variants constructed in this work will provide insight into the location and nature of the active site of this enzyme, thereby advancing our understanding of how hGOAT binds and octanoylates ghrelin.

Results and Discussion

Design of hGOAT truncation and loop variants

To identify which regions/domains of hGOAT are required for enzyme function, truncation mutants of hGOAT have been made that sequentially delete domains from the N-terminus of the protein. When designing the truncation mutants, the two conserved residues N307 and H338 located in the fourth "loop" (Figure 3) were taken into consideration. Mutation of these residues leads to loss of GOAT activity in the mouse-derived enzyme,[33] so loop D was maintained in all truncation constructs. The first truncation mutant, trunc2, deletes the first transmembrane helix and loop A (deletion of residues 1-42). Trunc3, the second truncation mutant, removes the first two helices along with loops A and B (deletion of residues 1-162) while the trunc4 variant (deletion of residues 1-240) eliminates helices 1-3 and loops A, B, and

C. Expressing these truncation mutants and assessing their ability to catalyze ghrelin acylation will indicate which domains of GOAT are necessary for enzyme stability and catalytic activity.
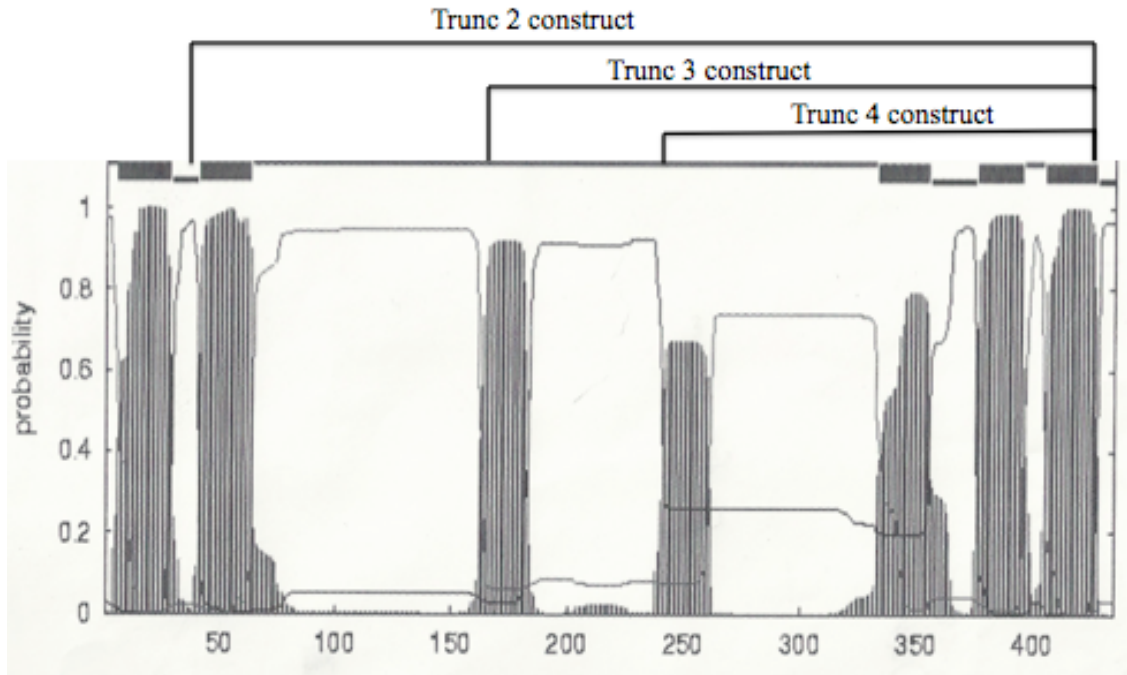
Figure 4. Design of hGOAT truncation mutants.[47]

In addition to truncation mutants, select loop regions were also cloned from the hGOAT sequence for expression (Figure 3). The loop regions were chosen based on TMHMM topology predictions and focused on loops of sufficient size (>40 amino acids) that the loops may fold independently. Based on these criteria, three loops regions were chosen: loop B (residues 62-162), loop C (184-240), and loop D (residues 262-344). The TMHMM algorithm also suggests the potential of one large loop domain within hGOAT, as indicated by the large BCD region in the center of the topology prediction (Figure 3). Based on this possibility, the combined region encompassing all three of these loops (loop BCD, residues 62-344) was also cloned from the parent hGOAT sequence for expression. These loops were cloned into bacterial expression vectors and their expression was attempted in *E. coli*, as described below.

Selection of positions for site-directed mutagenesis

To identify residues potentially involved in the hGOAT active site, several criteria were assessed. The first two positions selected for mutagenesis were Asn307 and His338, residues that are absolutely conserved residues across the MBOAT family.[33] Mutation of these residues in the mouse GOAT isoform led to a loss of enzyme activity, providing further evidence for their potential roles in GOAT catalysis.[33] Based on preliminary studies that suggest that hGOAT may require a metal ion for catalysis (Joseph Darling, unpublished data), we sought other conserved residues within loop D that could bind and position a catalytic metal ion. Mutations of potential metal binding ligands would disrupt the binding of the catalytic metal ion and would lead to a loss of enzyme activity. The four residues most commonly observed to bind and position catalytic metal ions in metalloenzymes are aspartic acid (D), glutamic acid (E), cysteine (C), and histidine (H).[48] Accordingly, the following conserved residues in loop D were mutated to alanine

to test for a loss of activity: H258, D262, D263, E281, E282, D287, D289, E294, D297, H338, H341, D358, and H361 (Figure 5). D358 nor H361 do not lie in loop D, but were mutated due to their close vicinity to loop D. It should be noted that all of these potential coordinating metal ligands lie within three amino acids of another potential metal ligand, consistent with structural motifs common to metalloenzymes.[49]
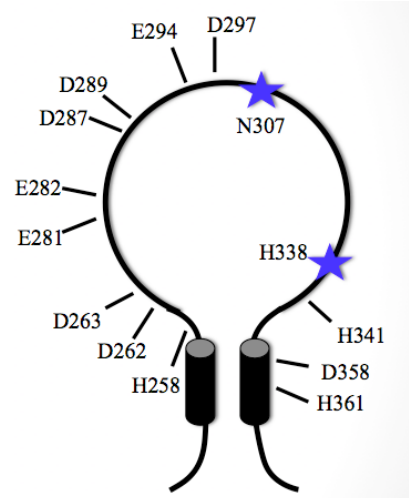
Figure 5. Potential metal ligands in loop D of hGOAT. The absolutely conserved residues N307 and H338 are noted by stars.

Studies of glycerol phosphate acyltransferases (GPATs), an enzyme family that performs a similar chemical reaction to ghrelin acylation by hGOAT, suggest another potential role for several of the conserved residues selected for mutation above. GPATs catalyze the first step in phospholipid biosynthesis by acylating the sn1 hydroxyl group of glycerol-3-phosphate.[50, 51, 52] Sequence comparisons within the GPAT family highlighted the conservation of an Hx_4D motif, and structural studies of squash chloroplast GPAT suggest that the histidine and aspartate within this motif are positioned to participate in catalysis.[50, 53, 54] The loss of enzyme activity upon site-directed mutagenesis of these residues in bacteria GPAT are consistent with these residues being involved in catalysis.[50, 53, 54] These studies suggest that the His and Asp in the Hx_4D work together in a manner similar to a serine protease, with the His residue acting as a base to deprotonate the hydroxyl group to promote nucleophilic attack on the acyl donor, while the Asp provides electrostatic and hydrogen-bonding stabilization to the transiently protonated His residue during catalysis.[50] Examination of the hGOAT sequence reveals a Hx_4D motif near the beginning of loop D composed of three residues (H258, D262, D263) which is highly conserved across GOAT isoforms (Figure 6). The similarity of the observed "HWILDD" motif to the Hx_4D motif from GPATs provides another mechanistic rationale for exploring the potential roles of these three residues in hGOAT catalysis of ghrelin acylation.

```
                           ↓      ↓
           HUMAN   YSHWILDDSLLHAAGFGPEL
     HOUSE MOUSE   YSHWILDDSLLHAAGFGAEA
       BROWN RAT   YSHWILDDSLLHAAGFGSEA
 AFRICAN ELEPHANT  YSHWVLDDSLLHAAGFGSEF
      CHIMPANZEE   YSHWILDDSLLHAAGFGPEL
      NWC GIBBON   YSHWILDDSLLHAAGFGPEL
   RHESUS MONKEY   YSHWILDDSLLHAAGFGSEL
  COMMON MARMOSET  YSHWILDDSLLYAAGFGSEL
           HORSE   YSHWILDDSLLCAAGFGSEF
    DOMESTIC DOG   YSCWILDDALLHAAGFGPGF
     GIANT PANDA   YSCWILDDALLQAAGFGPGF
     DOMESTIC COW  YSHWLLDDALLRAAGFGSEL
       WILD BOAR   YSHWILDESLLQAAGFGSGF
  RED JUNGLEFOWL   YSQWVLDEALLEAAGFGAAV
       ZEBRAFISH   YAHWKMSECVNNAAGLGVYF
```

Figure 6. Clustal-W alignment of GOAT sequences from various species illustrating the conservation of the HX_4D motif observed in glycerol phosphate acyltransferases.

PCR amplification to produce hGOAT truncation mutant constructs

Using the full-length hGOAT as a template, constructs were generated corresponding to the three planned truncation mutants using two-step PCR. The first PCR step cloned only the region of interest, while the second PCR step appended *EcoR*I and *Not*I restriction sites to the 5' and 3' ends of the truncation constructs to permit ligation of the constructs into expression vectors. A six amino acid leader sequence from hGOAT (Met-Glu-Trp-Lys-Trp) was also inserted at the 5'-end of the truncation constructs, as this sequence may be important for hGOAT membrane insertion.[55] Following the second PCR step, the lengths of the trunc2, trunc3, and trunc4 constructs were verified using agarose gel electrophoresis (Figure 7).

Figure 7. Analysis of hGOAT truncation constructs by agarose gel electrophoresis. The predicted sizes for the constructs are 1341 base pairs for Trunc2, 981 base pairs for Trunc3, and 747 base pairs for Trunc4.

Ligation of truncation mutant constructs into pFBD_MBOAT4

The truncation mutant construct were ligated into the pFBD_MBOAT4 vector, using the *EcoR*I and *Xba*I restriction sites to replace the full length hGOAT gene in this vector with the trunc2, trunc3, and trunc4 constructs. All truncation mutants were successfully ligated into pFBD_MBOAT4,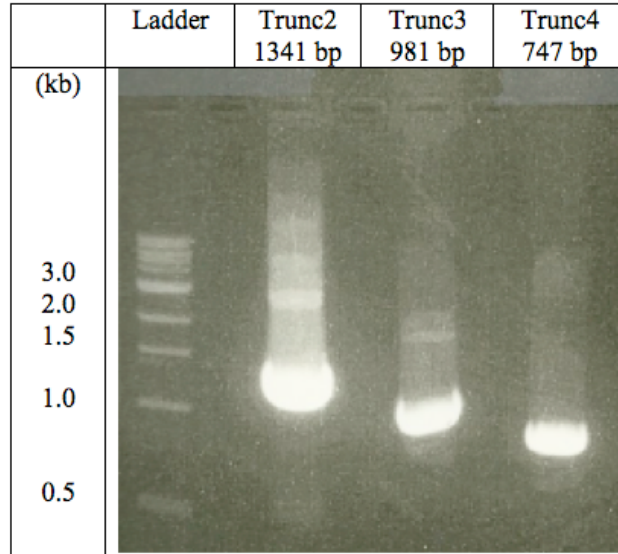 as verified by *Xho*I single and *EcoR*I / *Xba*I double restriction digests of the ligated plasmids (Figure 8). Successful ligation of the trunc2, trunc3, and trunc4 constructs into the pFBD vector adds a new *Xho*I site in addition to another *Xho*I site in the non-coding portion of the parent vector. Upon digestion by *Xho*I, the presence of these two *Xho*I sites will lead to generation of two linear DNA fragments whose sizes depend on the specific truncation construct (pFBD_trunc2 vector, 5013 and 1560 bp; pFBD_trunc3 vector, 4913 and 1200 bp; pFBD_trunc4 vector, 4913 and 966 bp). Double digestion of these vectors with *Xba*I and *EcoR*I should excise the truncation construct from the parent vector to yield two fragments (pFBD_trunc2 vector, 5188 and 1285 bp; pFBD_trunc3 vector, 5188 and 925 bp; pFBD_trunc4 vector, 5188 and 691 bp). Analytical digests of the pFBD_trunc2, pFBD_trunc3 vector, and pFBD_trunc4 vectors yielded the expected DNA fragments (Figure 8), consistent with successful ligations. The sequences of the truncation mutant plasmids were verified by DNA sequencing.

a.)

b.)

c.)
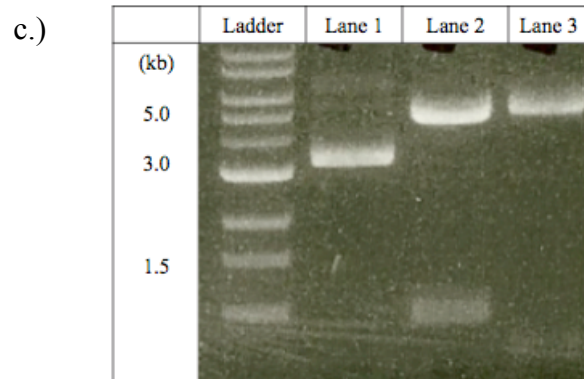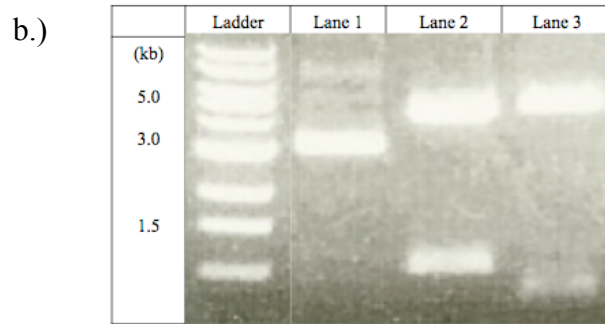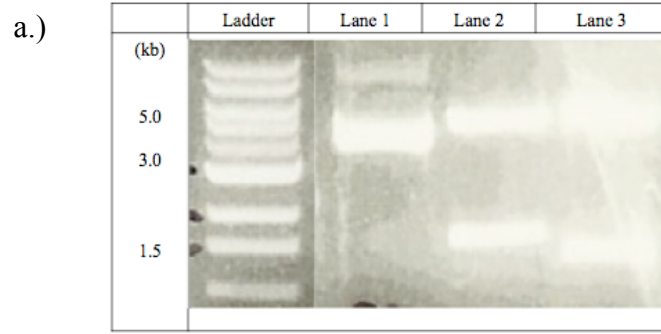
Figure 8. Analytical digests verifying ligations of the truncated mutants into pFBD_MBOAT4. a.) Digestion of pFBD_trunc2 vector. b.) Digestion of pFBD_trunc3 vector. c.) Digestion of pFBD_trunc2 vector. In all three gels, lane 1 is uncut pFBD_MBOAT4_truncation mutant vector, lane 2 is single digest with *Xho*1, and lane 3 is a double digest with *Xba*1 and *EcoR*1. All bands in the single and double digests match expected fragments as described in the text.

Generating recombinant baculovirus of the truncation mutants

The plasmids containing the truncation mutants (pFBD_trunc2, pFBD_trunc3, and pFBD_trunc4) were transformed into DH10Bac *E. coli* cells to generate recombinant bacmids for producing baculovirus. Plasmid transformation was selected for using the gentamicin resistance gene in the pFBD_MBOAT4 vector. Bacmids contain all of the genes necessary for expressing baculovirus in Sf9 insect cells and also contain a kanamycin resistance gene for bacterial selection. The DH10Bac *E. coli* cells contain a tetracycline resistant helper plasmid that expresses a transposase that inserts the target protein from the recombinant donor plasmid (e.g. pFBD_trunc2) into the bacmid using transposition sequences present in both the donor plasmid and bacmid (Figure 9). Blue/white screening and antibiotic selection were used to screen for colonies in which the gene for the GOAT truncation mutant successfully transposed into the bacmid. White colonies indicate a successful transposition as this transposition disrupts the lacZα (β-galactosidase) gene on the bacmid.[56]
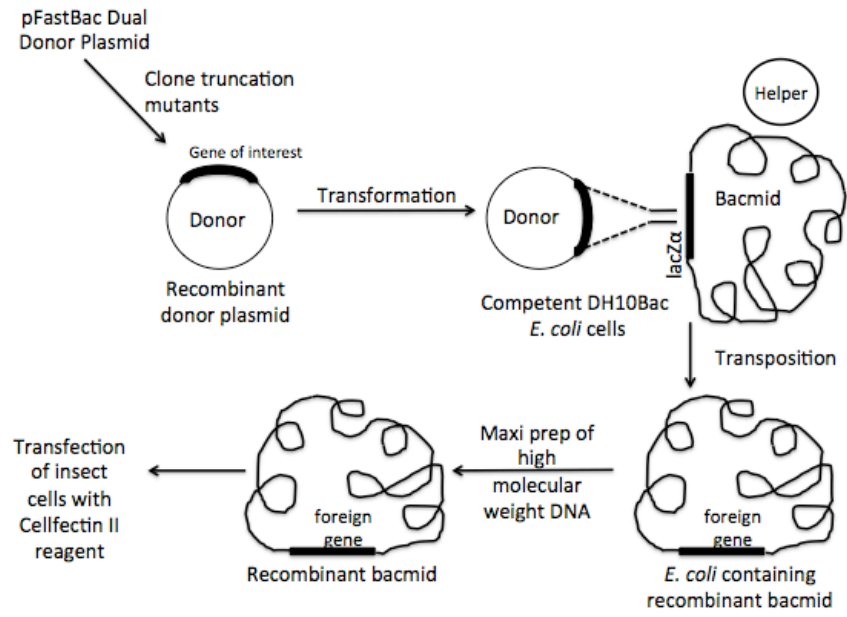
Figure 9. The Sf9 baculovirus expression system.[56]

As the bacmid is too large for analysis by gel electrophoresis (~135 kb), transposition of the target protein into the bacmid must be verified by PCR. PCR verified the bacmids were the proper size and that the recombinant donor plasmid was indeed transposed into the bacmid (Figure 10). In the event of successful transposition, the length of resulting PCR product includes bacmid sequence (2300 bp) and the size of the recombinant target gene inserted (Figure 10).[56] The expected sizes for the PCR products were 3901 bp for the trunc2 construct, 3541 bp for trunc3, and 3307 bp for trunc4.
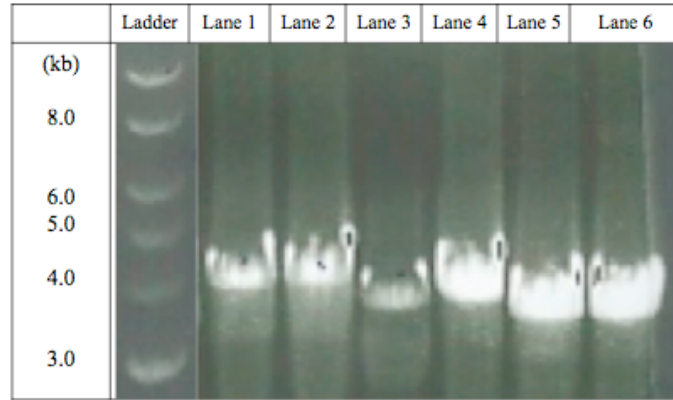
Figure 10. PCR verification of truncation construct bacmids. Lanes 1 and 2: trunc2 bacmid, with 30 ng (lane 1) or 100 ng (lane 2) of bacmid template; Lanes 3 and 4: trunc3 bacmid, with 30 ng (lane 3) or 100 ng (lane 4) of bacmid template; Lanes 5 and 6: trunc4 bacmid, with 30 ng (lane 5) or 100 ng (lane 6) of bacmid template. All PCR reactions yielded products with the expected sizes for successful bacmid construction.

Transfection of Sf9 insect cells with recombinant bacmid

Bacmid transfection into Sf9 insect cells leads to generation of recombinant baculovirus, which can subsequently be used to infect Sf9 insect cells for the expression of hGOAT truncation mutants. The initial transfection of bacmid into Sf9 cells is performed using a chemical reagent (Cellfectin reagent, Invitrogen), leading to viral expression and amplification that results in ~80% cell lysis over the course of 72 hours. The resulting baculovirus (passage 1 / P1 virus) is separated from cell debris by centrifugation, and is then used to infect fresh Sf9 cells to generate P2 virus. The P2 virus is then titered to determine viral concentration for subsequent protein expression. Expression of hGOAT mutant truncations was attempted by infecting Sf9 cells with P2 baculovirus followed by growth for 72 hours. The Sf9 membrane fractions are then collected to isolate the hGOAT mutant truncations as described in Materials and Methods.

Testing truncation mutants for ghrelin acylation by hGOAT

The membrane fractions from Sf9 cells infected with trunc2, trunc3, and trunc4 baculoviruses were probed for ghrelin acylation activity using a fluorescence-based assay developed in the Hougland lab.[46] The peptide substrate in this assay is a six amino-acid sequence derived from the N-terminal sequence of ghrelin (GSSFLS) with the C-terminal serine of this peptide (Ser 6) mutated to cysteine to allow chemoselective attachment of the fluorophore acrylodan (6-acryloyl-2-dimethylaminonapthalene) to form the GSSFLC$_{AcDan}$ substrate.[57, 58] GOAT-catalyzed octanoylation of serine 3 of this GSSFLC$_{AcDan}$ substrate leads to an increase in retention time.

a.)

b.)
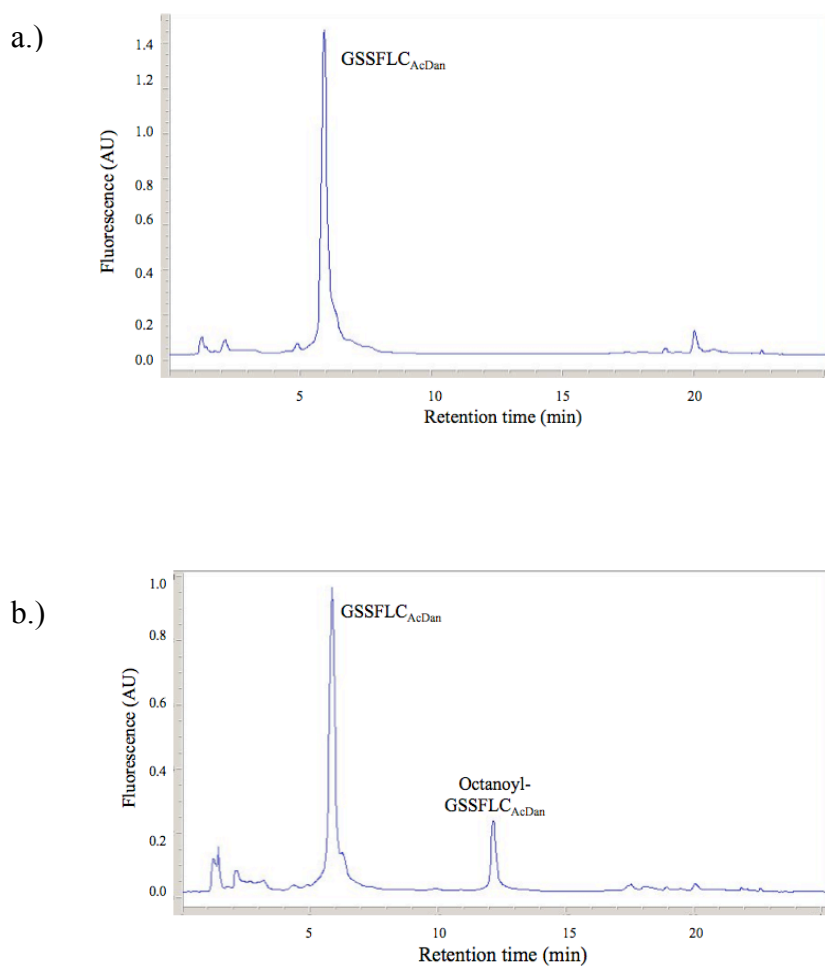
Figure 11. Octanoylation of GSSFLC$_{AcDan}$ by recombinant hGOAT. a.) Control reaction without octanoyl-CoA leaves GSSFLC$_{AcDan}$ unmodified (retention time 6 minutes). b.) GSSFLC$_{AcDan}$ acylation catalyzed by hGOAT membrane fraction in the presence of octanoyl-CoA, leading to the formation of octanoyl- GSSFLC$_{AcDan}$ (retention time 12 minutes). Figure adapted from reference.[46]

Similar to the unmodified enzyme, octanoylation activity by any of the truncation mutants should lead to formation of the peak for octanoyl- GSSFLC$_{AcDan}$ with a retention time of 12 minutes. However, none of membrane fractions from the truncation mutant expresssions exhibited octanoylation activity with the GSSFLC$_{AcDan}$ substrate (Figure 12). The lack of observed activity could arise from several factors. First, the enzyme truncation could lead to loss of enzyme activity through either disruption of the enzyme active site or overall enzyme destabilization. Second, as we are currently unable to detect the expression of hGOAT using Western blots or other analytical techniques, it is also possible that the truncation mutants were not efficiently expressed due to insufficient baculoviral infection during protein expression.
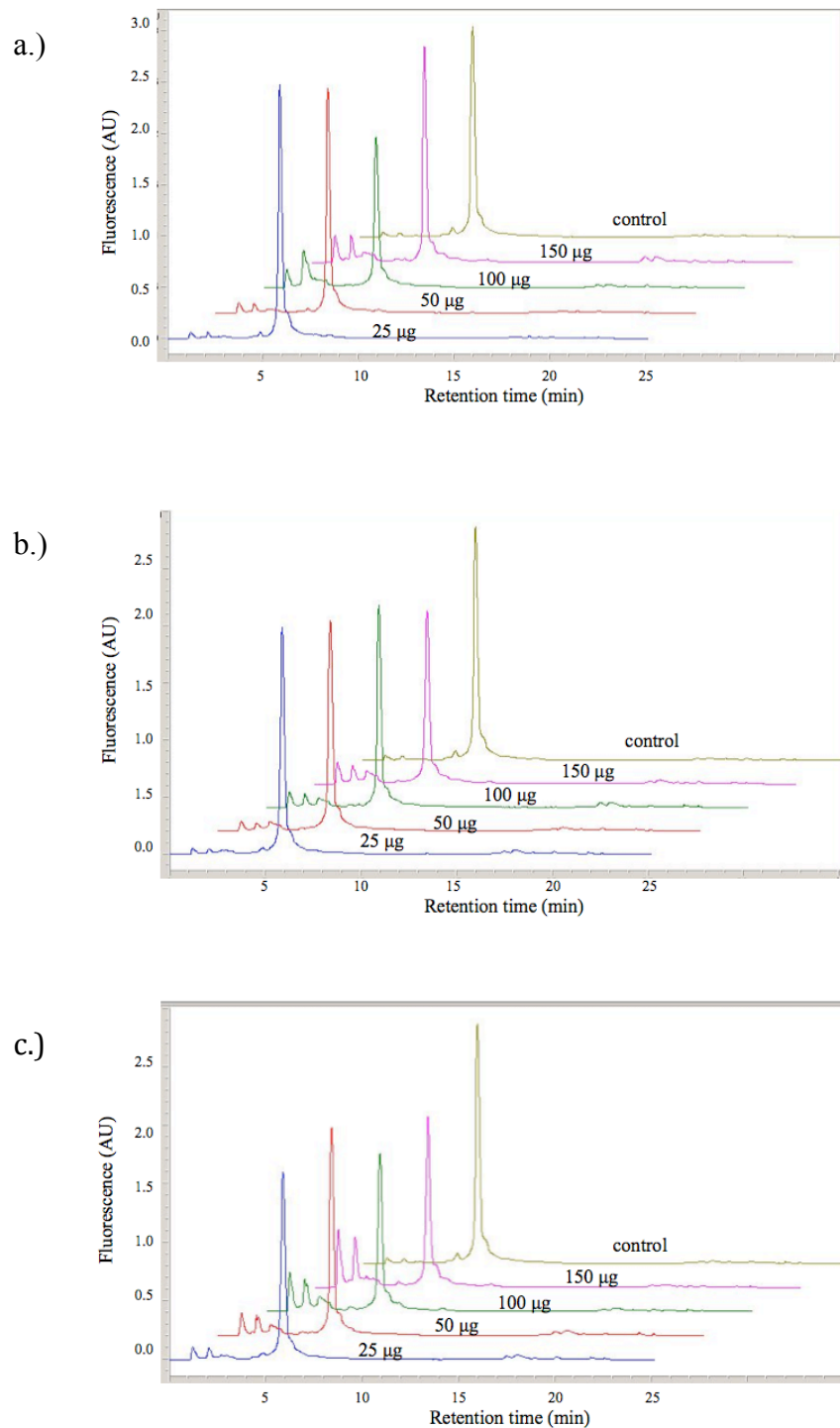
Figure 12. Octanoylation activity assays with hGOAT truncation mutants. a.) trunc2 mutant. b.) trunc3 mutant c.) trunc4 mutant. Assays were performed with 25 μg, 50 μg, 100 μg, and 150 μg of membrane protein from truncation mutant expressions and compared to a negative control reaction lacking octanoyl-CoA. Assays were performed as described in Materials and Methods.

Introduction of hGOAT mutations by PCR mutagenesis

Site-directed mutations within hGOAT were introduced by PCR mutagenesis using the

pFBD_MBOATi_FLAG plasmids as a template. At each targeted position, the natural amino

acid was mutated to alanine. Following mutagenesis and plasmid expression and purification,

the presence of the desired mutations were verified by DNA sequencing.

Using these plasmids containing the point mutants (pFBD_MBOATi_FLAG_H258A,

pFBD_MBOATi_FLAG_D262A, pFBD_MBOATi_FLAG_D263A,

pFBD_MBOATi_FLAG_E281A, pFBD_MBOATi_FLAG_E282A,

pFBD_MBOATi_FLAG_D287A, pFBD_MBOATi_FLAG_D289A,

pFBD_MBOATi_FLAG_E294A, pFBD_MBOATi_FLAG_D297A,

pFBD_MBOATi_FLAG_N307A, pFBD_MBOATi_FLAG_H338A,

pFBD_MBOATi_FLAG_H341, pFBD_MBOATi_FLAG_D358A,

pFBD_MBOATi_FLAG_H361A), bacmids for generation of mutant hGOAT baculovirus were

generated using transformation into DH10Bac *E. coli* cells as described above. Insertion of the

target hGOAT gene into the bacmid was verified by PCR (Figure 13). Four mutant plasmids did

not produce bacmid (H258A, D263A, D289A, and H341A) and will be retransformed into

DH10Bac *E. coli*. The verified hGOAT mutant bacmids will be transfected into Sf9 insect cells

and tested for ghrelin acylation activity by HPLC, following the same procedures done for the

truncation mutants.
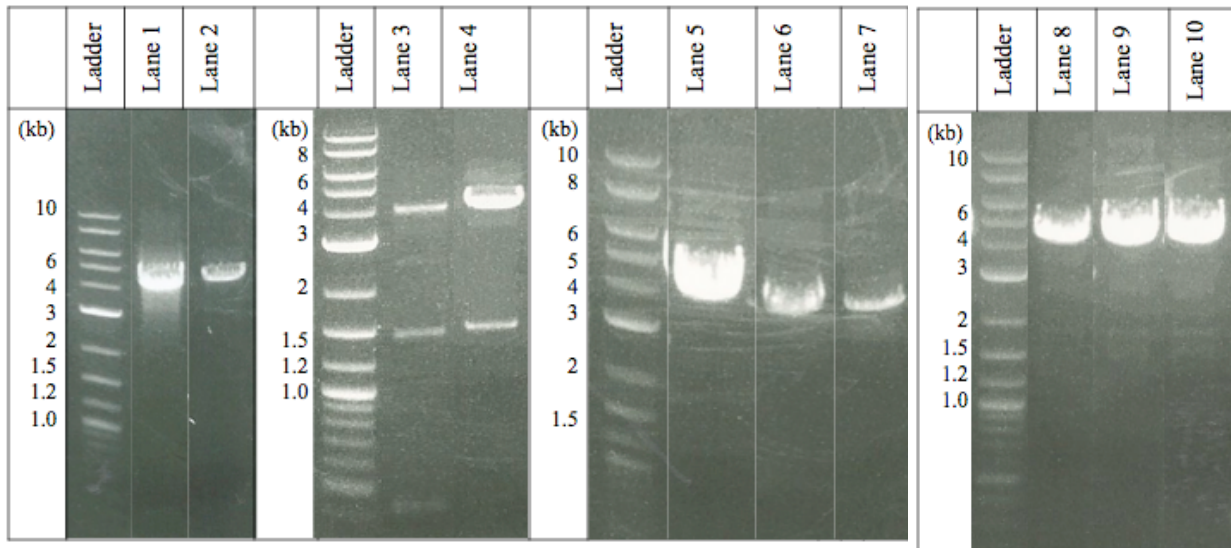
Figure 13. PCR verification of bacmids for hGOAT site directed mutants. Lane 1: H338A mutant; lane 2: H361A mutant; lane 3: D262A mutant; lane 4: D358A mutant; lane 5: E281A mutant; lane 6: E282A mutant; lane 7: D287A mutant; lane 8: E294A mutant; lane 9: D297A mutant; lane 10: N307A mutant. All bacmids with proper hGOAT gene insertions should yield a 4060 bp PCR product.

PCR amplification to construct isolated hGOAT loop domains

Constructs for hGOAT loops B, C, D, and BCD (as predicted by the TMHMM algorithm) were generated by PCR using full-length hGOAT as a template. The PCR cloned the region of interest and inserted *NdeI* and *HindIII* restriction sites to permit ligation into expression vectors. The lengths of loop B, loop C, loop D, and loop BCD were verified by agarose gel electrophoresis (Figure 14).
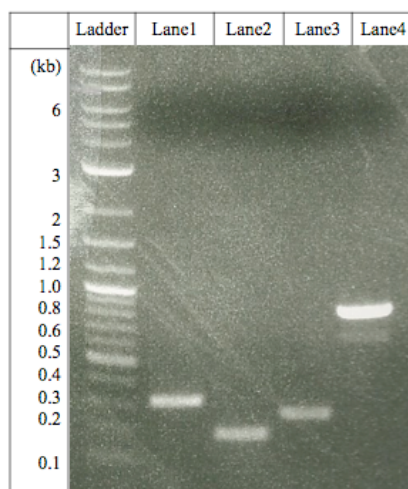
Figure 14. Agarose gel analysis of PCR reactions to generate hGOAT loop constructs. PCR product sizes were compared to a DNA standard ladder (far left). Lane 1: loop B, 327 bps; Lane 2: loop C, 183 bps; Lane 3: loop D, 261 bps; Lane 4: loop BCD, 858 bps.

Ligation of hGOAT loop constructs into pDB.His.MBP and pDB.GST vectors

To increase the solubility and stability of the hGOAT loops, we aimed to express them as fusion proteins coupled with either maltose binding protein (MBP) or glutathione S-transferase (GST). MDP and GST fusions are a common method employed to increase soluble expression of target proteins.[59] To generate these fusion protein constructs, the loop constructs were ligated into the pDB.His.MBP and pDB.GST vectors that contain MBP and GST, respectively. Loops C, D, and BCD were successfully ligated into the pDB.His.MBP, and loops B, D, and BCD were successfully ligated into pDB.GST, as verified by single (*NdeI*) and double (*NdeI*/ *HindIII*) restriction digests of the ligated plasmids (Figure 15).
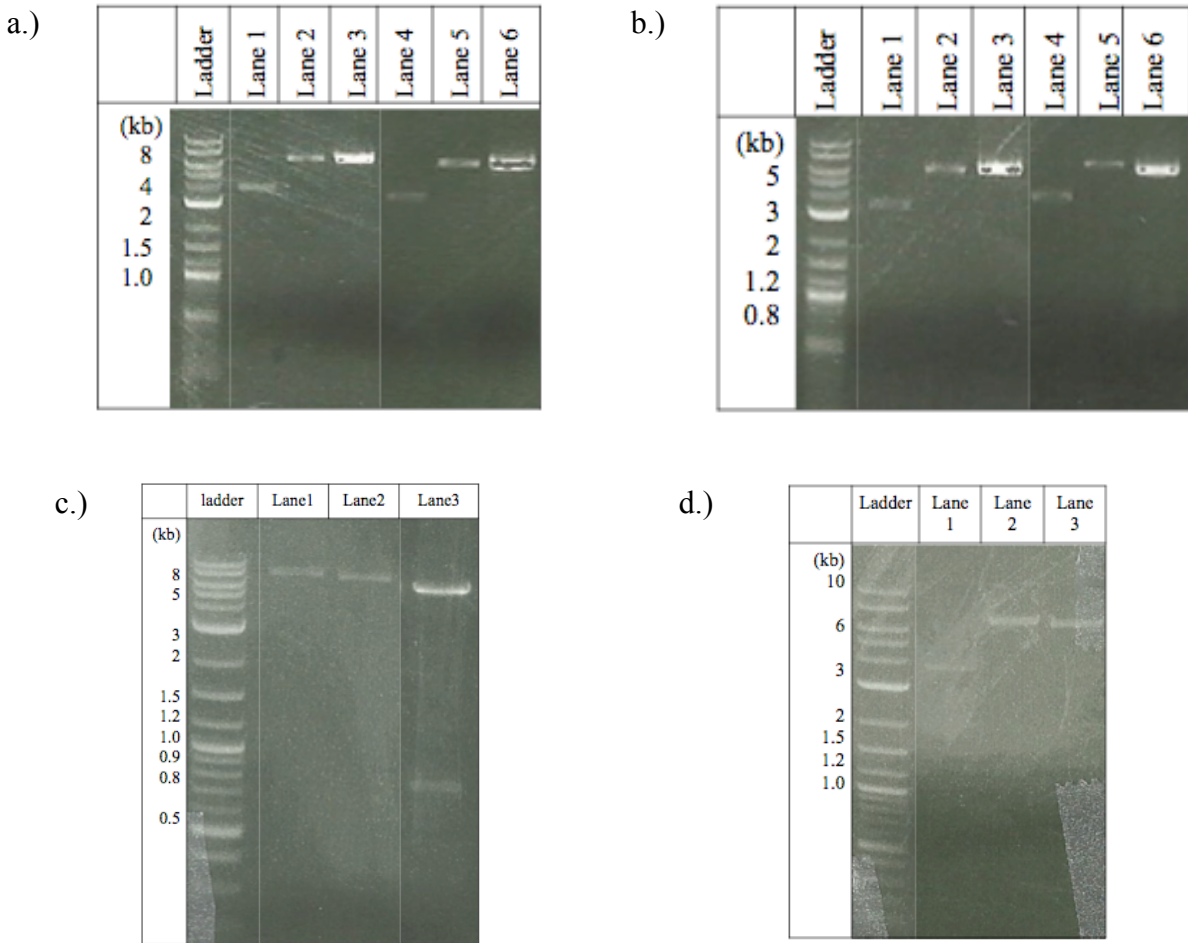
Figure 15. Restriction digests verifying ligation of hGOAT loop constructs into the pDB.His.MBP and pDB.GST vectors. a.) Lanes 1-3, pDB.His.MBP_loop D (lane 1 uncut, lane 2 *NdeI* single digest, lane 3 *NdeI* and *HindIII* double digest); Lanes 4-6, pDB.GST_loop B (lane 4 uncut, lane 5 *NdeI* single digest, lane 6 *NdeI* and *HindIII* double digest). b.) Lanes 1-3, pDB.GST_loop D (lane 1 uncut, lane 2 *NdeI* single digest, lane 3 *NdeI* and *HindIII* double digest); Lanes 4-6: pDB.GST_loop BCD (lane 4 uncut, lane 5 *NdeI* single digest, lane 6 *NdeI* and *HindIII* double digest). c.) pDB.His.MBP_loop BCD (lane 1 uncut, lane 2 *NdeI* single digest, lane 3 *NdeI* and *HindIII* double digest). d.) pDB.His.MBP_loop C (lane 1 uncut, lane 2 *NdeI* single digest, lane 3 *NdeI* and *HindIII* double digest).

The pDB.His.MBP- derived plasmids would be predicted to generate the following

fragments upon *Nde*I single digestion and double digestion with *Nde*I and *Hind*III:

pDB.His.MBP_loop C (single digestion 6607 bp, double digestion 6431 bp and 176 bp);

pDB.His.MBP_loop D (single digestion 6685 bp, double digestion 6431 bp and 254 bp);

pDB.His.MBP_loop BCD (single digestion 7285 bp, double digestion 6431 bp and 854 bp).

Similarly, the pDB.GST –derived plasmids would yield the following fragments upon *Nde*I

single digestion and double digestion with *Nde*I and *Hind*III: pDB.GST_loop B (single digestion

6271 bps, double digestion 5963 and 308 bps);. pDB.GST_loop D (single digestion 6217 bp,

double digestion 5963 and 254 bp); pDB.GST_loop BCD (single digestion 6817 bp, double

digestion 5963 and 854 bps). For each plasmid, the uncut vector runs at an apparent smaller size

due to supercoiling. The restriction digest results were consistent with predictions for each

plasmid, and the sequences of the loop construct fusion protein plasmids were verified by DNA

sequencing.

Expression trials for hGOAT loop fusion proteins

Following construction of the hGOAT loop fusion protein expression plasmids, we

attempted to express the fusion proteins using several different approaches. The fusion protein

plasmids (pDB.His.MBP_loop C, pDB.His.MBP_loop D, pDB.His.MBP_loop BCD,

pDB.GST_loop B, pDB.GST_loop D, and pDB.GST_loop BCD) were initially transformed into

BL21-DE3 *E.coli* cells for protein expression. For these trials, autoinduction media was used in

place of the classical method using IPTG induction of target protein expression.[59] In

autoinduction media, a mixture of glucose and lactose allows bacteria to grow to high density

using glucose as a carbon source followed by a switch to lactose metabolism when the glucose

supply is exhausted. The induction of lactose metabolism leads to galactose production, which can then bind to the *lac* repressor and induce expression of the target protein.[60]

The bacteria transformed with the hGOAT loop fusion protein plasmids were cultured in autoinduction media for 24 hours to allow for protein expression, as described in Materials and Methods. Bacteria were then harvested and analyzed for soluble protein expression by lysis and gel electrophoresis (Figure 16). The parent vectors pDB.His.MBP and pDB.GST gave robust expression of MBP (49 kDa) and GST (33kDa) as observed in lanes 1 and 5 of Figure 15, respectively. However, no new bands were observed at the predicted sizes for the loop fusion proteins (MBP-loop C, 54 kDa; MBP-loop D, 57 kDa; MBP- loop BCD, 79 kDa; GST-loop B, 43kDa; GST-loop D, 41 kDa; GST-loop BCD, 64 kDa). It appears that fusion to the hGOAT loop domains also blocked expression of MBP and GST, perhaps due to the lack of solubility of the loops or destabilization of MBP and GST folding. In the event that fusion to the hGOAT loop domains leads to protein insolubility, total cellular protein was analyzed in a 12% polyacrylamide gel by urea resolubilization of the insoluble pellet following cell lysis. However, this analysis did not provide any evidence for expression of the hGOAT loop fusion proteins.
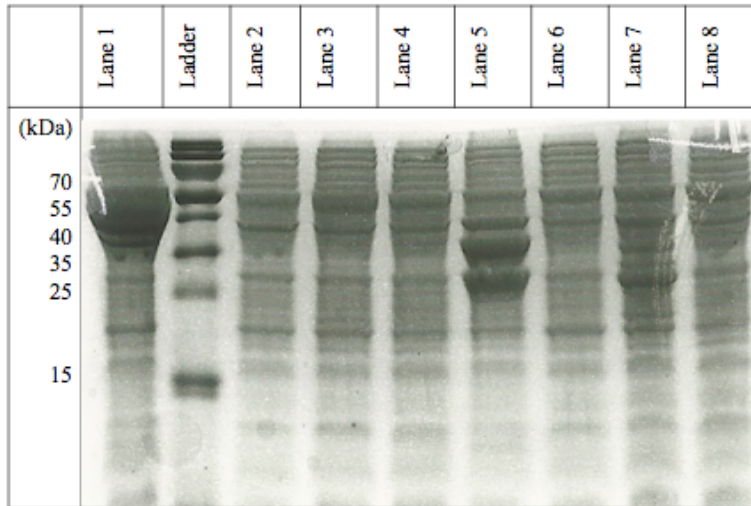
Figure 16.Analysis of hGOAT loop fusion protein expression using autoinduction media. Lane 1: pDB.His.MBP parent vector; lane 2: pDB.His.MBP_loop C; lane 3: pDB.His.MBP_loop D; lane 4: pDB.His.MBP_loop BCD; lane 5: pDB.GST parent vector; lane 6: pDB.GST_loop B; lane 7: pDB.GST_loop D; lane 8: pDB.GST_loop BCD.

Following unsuccessful expression of the hGOAT loop fusion proteins by auto-induction in BL21-DE3 cells, expression of the loops was attempted in Lemo21-DE3 *E. coli*. This strain of *E. coli* carries an auxiliary plasmid that allows lysozyme expression under the control of a rhamnose-inducible promoter.[61] Lysozyme serves as an inhibitor of the T7 RNA polymerase that is responsible for transcribing the mRNA for the target protein during IPTG-induced expression. Therefore, these bacteria allow for more control of target protein expression through titration with IPTG to induce protein expression and titration with rhamnose to control the activity of the T7 RNA polymerase. Studies have demonstrated that slower protein expression can lead to higher yields for proteins that are toxic or insoluble when expressed in *E. coli*.[61]

To validate the Lemo21-DE3 expression system, the pDB.His.MBP parent vector and pDB.His.MBP_loop BCD vectors were chosen. In these test expressions, IPTG and rhamnose were cross-titrated to sample the potential expression conditions, followed by protein expression analysis using gel electrophoresis (Figure 17). Cells transformed with the pDB.His.MBP parent vectors expressed MBP in presence of multiple IPTG concentrations without L-rhamnose added, while the addition of L-rhamnose effectively blocked MBP expression (Figure 17b). However, cells transformed with the pDB.His.MBP_loop BCD vector did not express either MBP-loop BCD (79 kDa) or MBP under any conditions tested (Figure 17c). This lack of expression is consistent with the expression trials using auto-induction in BL21-DE3 cells described above, suggesting that attachment of the hGOAT loop domains to MBP leads to protein instability. Varying trials were done in the Lemo21-DE3 cells, which included changing IPTG and L-rhamnose concentrations (0, 1.0, 1.5, and 2.0 mM L-rhamnose cross-titrated with 0, 0.2, 0.4, and 0.6 mM IPTG), incubation temperatures after initiation of induction (15 °C and 28 °C), and incubation time (2 hrs, 6 hrs, 8 hrs, and 58 hrs for the expressions growing at 15 °C). However,

none of the conditions attempted yielded detectible expression of the MBP-loopBCD fusion

protein.

a.)

		L-rhamnose Concentration (mM)			
		0	1.0	1.5	2.0
IPTG Concentration (mM)	0	1	2	3	4
	0.2	5	6	7	8
	0.4	9	10	11	12
	0.6	13	14	-	-

b.)

c.)
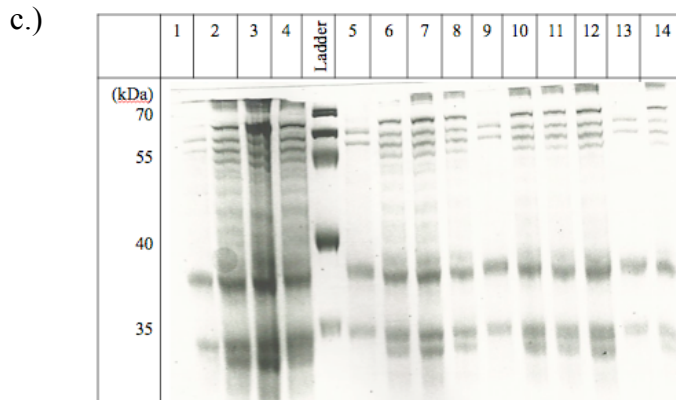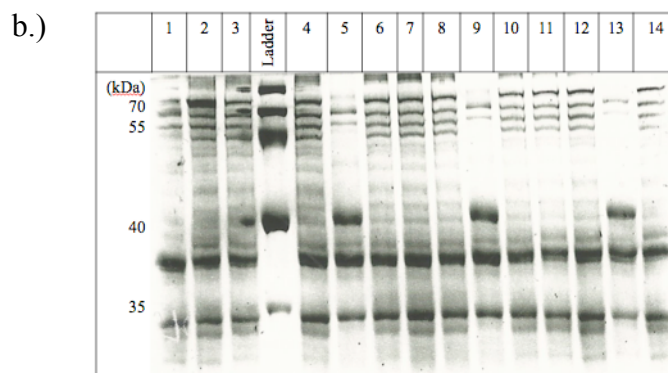
Figure 17. Expression of pDB.His.MBP and pDB.His.MBP_loop BCD in Lemo21-DE3 *E. coli*. a.) Cross-titration grid for varying IPTG L-rhamnose concentrations in test protein expression. The numbers in each cell of the table correspond to the conditions for the lane/culture of the same number in the gels in b) and c). b.) Analysis of pDB.His.MBP parent vector expression with IPTG and L-rhamnose cross-titration; c.) Analysis of pDB.His.MBP – loop BCD vector expression with IPTG and L-rhamnose cross-titration

Materials and Methods

Construction of hGOAT truncation mutants using two-step PCR

hGOAT truncation mutants were constructed using the pFastBacDual_MBOAT4 plasmid as template. Gene constructs for the truncation mutants were generated in two PCR steps. In this first step, a series of forward (5') primers were designed to anneal downstream of the domains to be deleted, with the reverse (3') primer used annealing at the C-terminus of the hGOAT gene. The reverse primer also installed a NotI restriction site at the 3' end of the truncated gene construct. Following amplification of the desired truncation mutant construct, a second PCR step was used to append a MEWLW leader sequence and *EcoR*I restriction site to the 5' end of the construct. The same reverse primer was used for all PCR reactions ((pUC57_Not1_subcloning): 5'-AGAGTT**GCGGCCGC**AGCTATGACCAT-3').

The forward primers used were as follows:

Table 1. Truncation mutant primers used for the first PCR.

Mutation	Primers
Trunc2	Forward: 5'-TTTCTTCTTACTGGTGGAGG-3'
Trunc3	Forward: 5'-CTTCCATATTTTTCTTATTTATTA-3'
Trunc4	Forward: 5'-ATTTATGTTGTATGGACAACTG-3'

Table 2. Truncation mutant primers used for the second PCR.

Mutation	Primers
Trunc2	Forward: 5'-AGTC**GAATTC**C*ATGGAGTGGCTTTGG*TTTCTTCTTACTGGTGGAGG-3'
Trunc3	Forward: 5'-AGTC**GAATTC**C*ATGGAGTGGCTTTGG*CTTCCATATTTTTCTTATTTATTA-3'
Trunc4	Forward: 5'-AGTC**GAATTC**C*ATGGAGTGGCTTTGG*ATTTATGTTGTATGGACAACTG-3'

PCR reactions (50 μL) consisted of One Taq DNA polymerase (0.5 μl, 2.5 units); dNTPs (1 μL of 1 mM stock); forward primer (1 μL of 10 μM stock); reverse primer (pUC57_Not1_subcloning, 1 μL of 10 μM stock); hGOAT template (pET24D_MBOAT4, 1 μL of 84 ng/μL stock), 5x One Taq standard reaction buffer (10 μL) and ultrapure H_2O (35.5 μL). The PCR thermocycler program proceeded as follows: initial denaturation (94 °C, 1 min); 30 cycles of denaturation (94 °C, 30 sec), annealing (56 °C, 1 min); and extension (68 °C, 2 min); final extension (68 °C, 5 min). PCR products were analyzed using agarose gel electrophoresis (0.8% agarose gel with 1X TAE buffer). Desired DNA bands were excised from the gel using EZ-10 Spin Column DNA Gel Extraction Kit (Bio Basic Inc.) following the manufacturer's instructions.

To insert *EcoR*1 and *Not*1 restriction sites at the 5' and 3'-terminii of the PCR-generated inserts for trunc2, trunc3, and trunc4, a second round of PCR was performed under the same conditions as described above using the DNA product isolated from the first PCR step as template DNA.

Double digestion of pFastBacDual vector and truncation mutants

Truncation mutant inserts and pFD_MBOAT4 vector (pFBD_MBOAT4) were digested with *EcoR*I and *Xba*I prior to ligation. The double digest reactions were performed under the following conditions: pFBD_MBOAT4 (70 μL total volume), pFBD_MBOAT4 (5 μg), *EcoR*I (1 μL, 20 units), *Xba*I (1 μL, 20 units), 100x BSA (0.7 μL), NEB 10x Buffer 4 (7 μL), and ultrapure H_2O (37.8 μL); Trunc2 (60 μL total volume), Trunc2 PCR product (1 μg), *EcoR*I (1 μL, 20 units), *Xba*I (1 μL, 20 units), 100x BSA (0.6 μL), NEB 10x Buffer 4 (6 μL), and ultrapure H_2O (35.4 μL); Trunc3 (50 μL total volume), Trunc3 PCR product (1 μg), *EcoR*I (1 μL, 20 units),

*Xba*1 (1 μL, 20 units), 100x BSA (0.5 μL), NEB 10x Buffer 4 (5 μL), and ultrapure H$_2$O (31.4 μL); Trunc4 (50 μL total volume), Trunc4 PCR product (1 μg), *EcoR*I (1 μL, 20 units), *Xba*I (1 μL, 20 units), 100x BSA (0.5 μL), NEB 10x Buffer 4 (5 μL), and ultrapure H$_2$O (29.1 μL). Reactions were incubated for 2 hours at 37 °C, followed by analysis and purification of the vector digestion by agarose gel electrophoresis (0.8% agarose, 1X TAE buffer); the size of the truncation inserts and linearized vector (4628 bp) were verified by comparison to a DNA standards ladder. The double digested truncation mutants PCR products were purified using the EZ-10 Column PCR Purification Kit (Bio Basic Inc.) per the manufacturer's instructions.

Ligation of truncation mutants into pFastBacDual vector

Ligations were performed using a 1:3 molar ratio of vector to insert. Ligation reactions were performed under the following conditions: Trunc2 construct (22 μL total volume), *EcoR*I-*Not*I double digested pFBD_MBOAT4 (31 ng), *EcoR*I-*Not*I double digested Trunc2 PCR product (26.9 ng), ultrapure H$_2$O (0.9 μL), 2x Quick Ligase buffer (10 μL), and T4 Quick Ligase (New England Biolabs, 1 μL); Trunc3 construct (21 μL total volume), *EcoR*I-*Not*I double digested pFBD_MBOAT4 (31 ng), *EcoR*I-*Not*I double digested Trunc3 PCR product (19.7 ng), ultrapure H$_2$O (2.2 μL), 2x Quick Ligase buffer (10 μL), and T4 Quick Ligase (New England Biolabs, 1 μL); Trunc4 construct (21 μL total volume), *EcoR*I-*Not*I double digested pFBD_MBOAT4 (31 ng), *EcoR*I-*Not*I double digested Trunc4 PCR product (15.0 ng), ultrapure H$_2$O (2.7 μL), 2x Quick Ligase buffer (10 μL), and T4 Quick Ligase (New England Biolabs, 1 μL). Following addition of Quick Ligase, reactions were incubated at room temperature for 5 minutes. Ligation mixtures (5 μL) were then transformed into a 50 μL aliquot of chemically competent Z-competent DH5α cells (Zymo Research) followed by incubation on ice for 30

49

minutes. Transformed bacteria were spread on LB-ampicillin plates (100 μg/mL) and incubated at 37 °C overnight.

Following overnight incubation at 37 °C, single colonies were inoculated into LB media (5 mL) containing ampicillin (100 μg/mL) in sterile culture tubes. These cultures were incubated overnight at 37 °C with shaking (225 RPM). Following overnight growth, plasmids were purified from the saturated cultures using EZ-10 Spin Column Plasmid DNA kit (Bio Basic Inc.) per manufacturer's instructions. Truncation inserts were verified by double digestion with *EcoR*I and *Xba*I to excise the ligated insert followed by agarose gel electrophoresis (Figure 7) and DNA sequencing (Genscript).

Construction of single-point hGOAT mutants

PCR mutagenesis primers were designed per manufacturer protocols (Strategene) and were synthesized by Integrated DNA Technologies (Table 1). Primers were dissolved in purified water and concentrations were measured by UV absorbance at 260 nm (1 OD = 50 ng/μL). PCR mutagenesis reactions (50 μL total volume) contained the following components: 10x *Pfu* reaction buffer (5 μL), pFBD_MBOATi_FLAG template (10 ng), forward primer (125 ng), reverse primer (125 ng), dNTPs (1 μL, 1 mM stock), and Pfu Turbo DNA polymerase (1 μL, Agilent). The thermocycler program for PCR mutagenesis proceeded as follows: initial denaturation (95 °C, 1 min); 18 cycles of denaturation (95 °C, 50 sec); annealing (60 °C, 50 sec); extension (68 °C, 12 min); and final extension (68 °C, 12 mins). Following PCR, reactions were digested with *Dpn*I (1 μL, 10 units) at 37 °C for 1 hour. After *Dpn*I digestion, the PCR reaction mixture (5 μL) were then transformed into a 50 μL aliquot of chemically competent Z-competent DH5α cells (Zymo Research) followed by incubation on ice for 30 minutes. Transformed bacteria were spread on LB-ampicillin plates (100 μg/mL) and incubated at 37 °C overnight.

Following overnight incubation at 37 $^{\circ}$C, single colonies were inoculated into LB media (5 mL) containing ampicillin (100 μg/mL) in sterile culture tubes. These cultures were incubated overnight at 37 °C with shaking (225 RPM). Following overnight growth, plasmids were purified from the saturated cultures using EZ-10 Spin Column Plasmid DNA kit (Bio Basic Inc.) per manufacturer's instructions. Single site mutations were verified by DNA sequencing (Genscript).

Table 3. Single point mutation quick-change mutagenesis primers used for the PCR.

Mutation	Primers
H258A	Forward: GCTGACCTACTACTCA**GCC**TGGATCCTCGACG
	Reverse: CGTCGAGGATCCAGGCTGAGTAGTAGGTCAGC
D262A	Forward: CACACTGGATCCTCGCCGATTCGCTCTTGC
	Reverse: GCAAGAGCGAATCGGCGAGGATCCAGTGTG
D263A	Forward: CTGGATCCTCGACGCTTCGCTCTTGCACG
	Reverse: CGTGCAAGAGCGAAGCGTCGAGGATCCA
E281A	Forward: GACAGTCACCAGGA**GCG**GAAGGTTACGTTCC
	Reverse: GGAACGTAACCTTCCGCTCCTGGTGACTGTC
E282A	Forward: GTCACCAGGAGAG**GCA**GGTTACGTTCCTG
	Reverse: CAGGAACGTAACCTGCCTCTCCTGGTGAC
D287A	Forward: GGTTACGTTCCT**GCC**GCTGATATCTGGACC
	Reverse: GGTCCAGATATCAGCGGCAGGAACGTAACC
D289A	Forward: CGTTCCTGACGCT**GCT**ATCTGGACCCTGG
	Reverse: CCAGGGTCCAGATAGCAGCGTCAGGAACG
E294A	Forward: GATATCTGGACCCTG**GCA**AGGACTCACAGAATC
	Reverse: GATTCTGTGAGTCCTTGCCACGGTCCAGATATC
H297A	Forward: CCCTGGAAAGGACT**GCC**AGAATCTCGGTCTTC
	Reverse: GAAGACCGAGATTCTGGCAGTCCTTTCCAGGG
N307A	Forward: CTCCCGTAAGTGG**GCC**CAAAGCACTGCTCGC
	Reverse: GCGAGCAGTGCTTTGGGCCCACTTACGGGAG
H338A	Forward: CAGCTTGGTGG**GCC**GGACTGCACCCTGG
	Reverse: CCAGGGTGCAGTCCGGCCCACCAAGCTG
H341A	Forward: GCACGGACTG**GCC**CCTGGACAGGTTTTCGG
	Reverse: CCGAAAACCTGTCCAGGGGCCAGTCCGTGC
D358A	Forward: GTTATGGTGGAGGCC**GCC**TACCTGATCCAC
	Reverse: GTGGATCAGGTAGGCGGCCTCCAGCATAAC
H361A	Forward: GCCGACTACCTGATC**GCC**TCCTTCGCTAACGAG
	Reverse: CTCGTTACGGAAGGAGGCGATCAGGTAGTCGGC

Generation of recombinant baculovirus using pFastBacDual vectors

To generate bacmid for transfecting into Sf9 insect cells, pFastBacDual vectors were transformed into DH10Bac *E. coli* cells by adding chilled plasmid (100 ng) to an aliquot of Z-competent DH10Bac cells (50 μL), followed by incubation on ice for 15 minutes. The transformed bacteria were then spread onto LB agar plates containing kanamycin (50 μg/mL), tetracycline (10 μg/mL), gentamicin (7 μg/mL), IPTG (40 μg/mL), and XGal (100 μg/mL). Plates were incubated at 37 °C for 48 hours, at which point bacteria with successful bacmid recombination were identified by blue/white screening. White colonies were re-streaked onto LB agar plates containing kanamycin, tetracycline, gentamicin, IPTG, and XGal and incubated for 48 hours at 37 °C to verify bacmid recombination by blue/white screening. White colonies from the second blue/white screening were inoculated into 5 mL LB cultures containing kanamycin (50 mg/mL), gentamicin (10 mg/mL), and tetracycline (5 mg/mL) to amplify bacmids containing MBOAT sequences. Following initial growth of 5 mL cultures at 37 °C with shaking (225 rpm) for 7 hours, the total volume of the initial culture was used to inoculate a 500 mL culture in a 2 L sterile flask (500 mL LB media, kanamycin (50 mg/mL), gentamicin (10 mg/mL), and tetracycline (5 mg/mL). These 500 ml cultures were incubated at 37 °C with shaking (175 rpm) overnight. Following overnight incubation, bacmids were purified using Nucleobond Bac 100 maxi purification kit (Macherey-Nagel) per the manufacturer's instructions and stored at 4 °C.

Following purification, bacmid samples were prepared for transfection in tissue culture to generate baculovirus. To generate P1 virus, Grace's basal media (Cellgro, 4 mL) was added to T25 flasks and inoculated with a volume of 8×10^6 sf9 insect cells (1 mL). Following cell addition, flasks were incubated at room temperature for 30 minutes to allow cell attachment. During this incubation, solutions of Cellfectin II reagent (Invitrogen, 20 μL) in Grace's basal

media (230 μL, total volume 250 μL) and bacmid (2 μg) in Grace's basal media (250 μL) were prepared. These solutions were then combined and incubated at room temperature for 30 minutes. The combined solution was added dropwise to the T25 flasks containing Sf9 cells, followed by incubation at 27 °C for 4 hours. The transfection media was then removed from the Sf9 cells and replaced with 5 mL of Sf9 Insectagrow (Cellgro), followed by cell incubation at 27 °C until 80% cell lysis is observed (~96 hours total incubation).

Baculovirus (P1 virus) was harvested from the transfected cells by transferring media from the T25 flasks to 15 ml conical tubes, followed by centrifugation (500 x g, 5 minutes) to pellet cellular debris. The supernatant containing the P1 virus was then transferred to new sterile conical tubes and stored at 4 °C.

To produce P2 virus, a volume of 2 x 10^6 cells/ mL(7 mL) was combined with P1 virus (2 mL) and 41 mL of Insectagro growth media for a total of 50 mL and incubated at 27 °C for 96 hours. Following incubation, P2 virus is syringe filtered with a 0.45 μM syringe and stored in a 50 mL conical tube at 4 °C.

P2 baculoviral concentration (titer, pfu/mL) was determined with the FastPlax Titer Kit (Novagen) per manufacturer's instructions. For P2 stocks with concentrations below that needed for protein expression, the P2 baculovirus was concentrated by ultra-centrifugation (80,000 x g, 60 minutes). The pellet for each P2 stock was resuspended in sufficient Insectagro media to generate baculoviral stocks at sufficient titer for protein expression (10 pfu/mL); pellet resuspension requires storage of the media and viral pellets at 4 °C for 5 days.

Baculoviral Expression of MBOAT and MBOAT variants

For protein expression, Sf9 insect cell cultures (1×10^6 cell/mL) were infected with P2 baculovirus at a multiplicity of infection (MOI) of 10; culture volumes were determined by the amount of P2 virus available (e.g. Trunc2: 100 mL culture; Trunc3: 12 mL culture; Trunc4: 80 mL culture). Cultures were infected with P2 virus and incubated at 27 °C with stirring (150 rpm) for 72 hours.

Membrane fraction enrichment from Sf9 insect cells

Following protein expression, Sf9 cultures were harvested by centrifugation (500 x g, 5 minutes) at 4 °C. Cell pellets were resuspended in 1/20 culture volume of lysis buffer [150 mM NaCl, 50 mM Tris-HCl pH 7.0, 1 mM NaEDTA, 1 mM DTT, complete mini-tab protease inhibitor (Roche Pharmaceuticals), 10 µg/mL Pepstatin A, 100 µM bis (4-nitrophenyl) phosphate]. The resuspended cells were transferred to a dounce homogenizer and lysed by 40 dounce strokes on ice, followed by removal of cell debris by centrifugation (3000 x g, 5 minutes) at 4 °C. The membrane protein fraction was isolated from the resulting supernatant by ultracentrifugation (100,000 x g, 1 hour) at 4 °C. The isolated membrane fraction pellet was resuspended in buffer (50 mM HEPES, pH 7.0) by pipetting (25 strokes). Protein concentration was determined by Bradford assay (Bio-Rad, Hercules, CA), and the resuspended membrane fractions were aliquoted (50 µL) and stored at -80 °C until use.

hGOAT activity assay

Membrane fractions from Sf9 cells expressing hGOAT variants were thawed on ice and passed through an 18 gauge needle ten times. Membranes were then centrifuged (1000 x g, 1 min), with the supernatant collected and added to hGOAT reactions. Reactions contained the desired concentration of membrane fraction as determined by Bradford assay (25 μg, 50 μg, 100 μg, or 150 μg). Unless noted otherwise, assays were performed with 1.5 μM acrylodanylated peptide substrate (GSSFLC$_{AcDan}$), 500 μM octanoyl-CoA, and 50 mM HEPES pH 7.0 in a total volume of 50 mL. Assays were initiated by addition of the acrylodanylated peptide substrate. Assays were incubated at room temperature and stopped by addition of 50 μL of 20% acetic acid in isopropanol. Assays were analyzed by reverse phase HPLC (Zorbax Eclipse XDB column, 4.6 x 150 mm) using a gradient from 30% acetonitrile in water containing 0.05% TFA to 63% acetonitrile in water containing 0.05% TFA flowing at 1 mL/min over 14 min, followed by 100% acetonitrile for 5 min; acrylodanylated peptides were detected by UV absorbance at 360 nm and fluorescence (l$_{ex}$ 360 nm, l$_{em}$ 485 nm). Peptide substrates typically eluted with a retention time of 5-7 minutes, with the octanoylated peptide product eluting at ~12 min. Chromatogram analysis and peak integration was performed using Chemstation for LC (Agilent Technologies).

Construction of hGOAT loop mutants constructs

Constructs for the predicted soluble loops within hGOAT (loops B, C, D, and BCD) were generated by PCR amplification of the corresponding regions within the pUC57 MBOAT4 vector. The forward (5') primers anneal upstream of the desired loop region and install a *Nde*I restriction site at the 5'-end of the PCR product. Similarly, the reverse (3') primers anneal downstream of the desired region and install a 3' *HindIII* restriction site. For the BCD loop

region, the loop B forward and loop D reverse primers were used. The primers used were as

follows (restriction sites noted in bold):

Table 4. Loop mutation primers used for the PCR.

Mutation	Primers
Loop B	Forward: 5'-TCGATC**CATATG**TTAGTATTTACTCCAGCAGTTT-3' Reverse: 5'-GATCGA**AAGCTT**AGCTTTACAAACATGTTCACTC-3'
Loop C	Forward: 5'-TCGATC**CATATG**CAACGATTTCAAGCTCGTGTT-3' Reverse: 5'-GATCGA**AAGCTT**ACATTCAAATTGTTGACAATCAG-3'
Loop D	Forward: 5'-TCGATC**CATATG**GATGATTCACTTTTGCATGCTG-3' Reverse: 5'-GATCGA**AAGCTT**TTGACCAGGATGTAATCCATC-3'
Loop BCD	Forward: 5'-TCGATC**CATATG**TTAGTATTTACTCCAGCAGTTT-3' Reverse: 5'-GATCGA**AAGCTT**TTGACCAGGATGTAATCCATC-3'

PCR reactions (50 μL) consisted of One Taq DNA polymerase (0.5 μL, 2.5 units); dNTPs (1 μL of 1 mM stock); forward primer (1 μL of 10 μM stock); reverse primer (1 μL of 10 μM stock); pUC57_MBOAT4 template (60 ng), 5x One Taq standard reaction buffer (10 μL) and ultrapure H_2O (35.5 μL). The PCR thermocycler program proceeded as follows: initial denaturation (94 °C, 1 min); 30 cycles of denaturation (94 °C, 30 sec), annealing (56 °C, 1 min); and extension (68 °C, 2 min); final extension (68 °C, 5 min). PCR products were analyzed using agarose gel electrophoresis (0.8% agarose gel with 1X TAE buffer). Desired DNA bands were excised from the gel using EZ-10 Spin Column DNA Gel Extraction Kit (Bio Basic Inc.) following the manufacturer's instructions.

Double digestion of pDB.His.MBP and pDB.GST vectors and loop mutants

hGOAT loop mutant inserts (loop B, loop C, loop D, loop BCD) and fusion protein expression vectors (pDB.His.MBP and pDB.GST) were digested with *Nde*I and *Hind*III prior to ligation. The double digest reactions were performed under the following conditions: pDB.His.MBP (total volume 40 μL), pDB.His.MBP (3 μg), *Nde*I (1 μL, 20 units), *Hind*III (1 μL, 20 units), 100x BSA (0.4 μL), NEB 10x Buffer 2 (4 μL), and ultrapure H_2O (22.7 μL); pDB.GST (total volume 40 μL), pDB.GST (3 μg), *Nde*I (1 μL, 20 units), *Hind*III (1 μL, 20 units), 100x BSA (0.4 μL), NEB 10x Buffer 2 (4 μL), and ultrapureH_2O (25.3 μL); loop B (total volume 60 μL), loop B PCR product(1 μg), *Nde*I (1 μL, 20 units), *Hind*III (1 μL, 20 units), 100x BSA (0.6 μL), NEB 10x Buffer 2 (6 μL), and ultrapure H_2O (33.2 μL); loop C (total volume 60 μl); loop C PCR product (1 μg), *Nde*I (1 μL, 20 units), *Hind*III (1 μL, 20 units), 100x BSA (0.6 μL), NEB 10x Buffer 2 (6 μL), and ultrapure H_2O (35.4 μL); loop D (total volume 70 μL), loop D PCR product (1 μg), *Nde*I (1 μL, 20 units), *Hind*III (1 μL, 20 units), 100x BSA (0.7 μL), NEB 10x

Buffer 2 (7 µL), and ultrapure H_2O (37.2 µL; loop BCD (total volume 50 µL), loop BCD PCR product (1 µg), *Nde*I (1 µL, 20 units), *Hind*III (1 µL, 20 units), 100x BSA (0.5 µL), NEB 10x Buffer 2 (5 µL), and ultrapure H_2O (30 µL).

Reactions were incubated for 2 hours at 37 °C, followed by analysis of the vector digestions by agarose gel electrophoresis (0.8% agarose, 1X TAE buffer) to verify the size of the linearized pDB.His.MBP and pDB.GST vectors (6431 and 6963 bp, respectively). The digested vectors were purified using an EZ-10 Spin Column DNA Gel Extraction Kit (Bio Basic Inc.) per the manufacturer's instructions. The double digested loop PCR product inserts were purified using the EZ-10 Column PCR Purification Kit (Bio Basic Inc.) per the manufacturer's instructions.

Ligation of loop mutants into pDB.His.MBP and pDB.GST vectors

Ligations were performed using a 1:3 molar ratio of vector to insert. Ligation reactions were performed under the following conditions: Loop C and pDB.His.MBP construct (24 µL total volume), *Hind*III-*Nde*I double digested pDB.His.MBP (18.7 ng), *Hind*III-*Nde*I double digested loop C PCR product (1.58 ng), ultrapure H_2O (7.1 µL), 2x Quick Ligase buffer (10 µL), and T4 Quick Ligase (New England Biolabs, 1 µL); Loop D and pDB.His.MBP construct (24 µL total volume), *Hind*III-*Nde*I double digested pDB.His.MBP (18.7 ng), *Hind*III-*Nde*I double digested loop D PCR product (2.25 ng), ultrapure H_2O (7.1 µL), 2x Quick Ligase buffer (10 µL), and T4 Quick Ligase (New England Biolabs, 1 µL); Loop BCD and pDB.His.MBP construct (24 total volume), *Hind*III-*Nde*I double digested pDB.His.MBP (18.7 ng), *Hind*III-*Nde*I double digested loop BCD PCR product (7.41 ng), ultrapure H_2O (3.1 µL), 2x Quick Ligase buffer (10 µL), and T4 Quick Ligase (New England Biolabs, 1 µL); Loop B and pDB.GST construct (22 µL

total volume), *Hind*III-*Nde*I double digested pDB.GST (12 ng), *Hind*III-*Nde*I double digested

loop B PCR product (2 ng), ultrapure H_2O (2.1 μL), 2x Quick Ligase buffer (10 μL), and T4

Quick Ligase (New England Biolabs, 1 μL); Loop D and pDB.GST construct (22 μL total

volume), *Hind*III-*Nde*I double digested pDB.GST (12 ng), *Hind*III-*Nde*I double digested loop D

PCR product (1.6 ng), ultrapure H_2O (2.1 μL), 2x Quick Ligase buffer (10 μL), and T4 Quick

Ligase (New England Biolabs, 1 μL); Loop BCD and pDB.GST construct (22 μL total volume),

*Hind*III-*Nde*I double digested pDB.GST (12 ng), *Hind*III-*Nde*I double digested loop BCD PCR

product (5.1 ng), ultrapure H_2O (1.1 μL), 2x Quick Ligase buffer (10 μL), and T4 Quick Ligase

(New England Biolabs, 1 μL). Following addition of Quick Ligase, reactions were incubated at

room temperature for 5 minutes. Ligation mixtures (5 μL) were then transformed into a 50 μL

aliquot of chemically competent Z-competent DH5α cells (Zymo Research) followed by

incubation on ice for 30 minutes. Transformed bacteria were spread on LB-ampicillin plates (100

mg/mL) and incubated at 37 °C overnight.

Following overnight incubation at 37 °C, single colonies were inoculated into LB media

(5 mL) containing ampicillin (100 μg/mL) in sterile culture tubes. These cultures were incubated

overnight at 37 °C with shaking (225 RPM). Following overnight growth, plasmids were purified

from the saturated cultures using EZ-10 Spin Column Plasmid DNA kit (Bio Basic Inc.) per

manufacturer's instructions. Truncation inserts were verified by double digestion with *Hind*III

and *Nde*I to excise the ligated insert followed by agarose gel electrophoresis (Figure 13) and

DNA sequencing (Genscript).

Expression of hGOAT loop fusion proteins using autoinduction media

Plasmids encoding the hGOAT loop fusion proteins (pDB.His.MBP_loop C, pDB.His.MBP_loop D, pDB.His.MBP_loop BCD, pDB.GST_loop B, pDB.GST_loop D, pDB.GST_loop BCD) were transformed into BL21 (DE3) *E. coli* cells. Plasmids (100 ng) were transformed into a 50 μL aliquot of chemically competent Z-competent BL21 (DE3) cells (Zymo Research) followed by incubation on ice for 30 minutes. Transformed bacteria were spread on LB-kanamycin plates (50 μg/mL) and incubated at 37 °C overnight.

Following overnight incubation, single colonies were used to inoculate 1 mL culture of autoinduction media (1% tryptone, 0.5% yeast extract, 25 mM Na_2HPO_4, 25 mM KH_2PO_4, 50 mM NH_4Cl, 5 mM Na_2SO_4, 2 mM $MgSO_4$, 0.2x trace metals (0.01 mM $FeCl_3$, 0.004 mM $CaCl_2$, 0.002 mM $MnCl_2$ $7H_2O$, 0.002 mM $ZnSO_4$ $7H_2O$), 0.5% glycerol, 0.05% glucose, 0.2% α-D-lactose, and 50 μg/mL kanamycin) in one well of a 96-deep well plate. The plates were sealed with gas permeable seals (Thermo Scientific) and shaken for 24 hours at 400 rpm at 28 °C. Following growth, bacteria were harvested by centrifugation (6000 x g, 15 min) and the supernatant removed. The bacterial pellet was resuspended in B-PER lysis reagent (Thermo Scientific, 150 μL), vortexed on high for 1 min, and cell debris was removed by centrifugation (15,000 x g ,5 mins). Proteins in the resulting supernatant were then analyzed 12% acrylamide gel electrophoresis and Coomassie staining (Figure 14).

Expression of hGOAT loop fusion proteins using Lemo21 E. coli

The pDB.His.MBP parent vector and pDB.His.MBP_loop BCD were transformed into Z-competent Lemo21(DE3) *E. coli* cells. Plasmids (100 ng) were added to 50 μL aliquots of Z-competent Lemo21(DE3) *E. coli*, followed by incubation on ice for 30 min. Following

incubation on ice, SOC media (200 μL) was added and transformations were shaken for 2 hours at 225 rpm for 2 hours at 37 °C. The entire volume of the transformation was spread onto LB agar plates containing kanamycin (50 μg/mL) and chloramphenicol (20 μg/mL) and incubated overnight at 37 °C.

Following overnight incubation, single colonies were inoculated into 5 mL cultures of LB media containing kanamycin (50 μg/mL) and chloramphenicol (20 μg/mL). These cultures were incubated at 37 °C approximately 2 hours until slight turbidity was evident (OD_{600} ~0.1). Expression cultures consisting of 50 mL of 2xYT media with kanamycin (50 μg/mL) and chloramphenicol (20 μg/mL) were inoculated with 1 mL of the starter cultures, followed by incubation with shaking at 225 RPM at 37 °C until cultures reached an OD_{600} of 0.6-0.8. Once the cultures reached the desired optical density, the cultures were split into 1 mL aliquots and varying amounts of IPTG and L-rhamnose were titrated into each 1 mL cultures contained in a 96-deep well plate to induce protein expression. The plates were then sealed with gas permeable seals (Thermo Scientific) and shaken at 225 rpm for 6 hours at 37 °C. Following growth and induction, bacteria were harvested by centrifugation (6000 x g, 10 min) and the resulting cell pellets were stored at -80 °C until expression analysis by cell lysis and gel electrophoresis followed by Coomassie staining (Figure 16).

CHAPTER THREE

CHARACTERIZING THE ACYL DONOR SPECIFICITY OF HUMAN GHRELIN O-
ACYLTRANSFERASE

Introduction

A number of different acyl modifications of ghrelin by hGOAT besides octanoylation were screened for activity to test the specificity of hGOAT modification. The initial isolation and identification of ghrelin revealed the presence of an octanoyl (C8 fatty acid) group attached to serine 3 of ghrelin.[1] In the initial study identifying ghrelin O-acyltransferase (GOAT), Yang and coworkers reported that GOAT accepted octanoyl-CoA as the acyl donor for ghrelin modification.[33] GOAT was also shown to be able to catalyze transfer of this octanoyl group from octanoyl CoA to a mock ghrelin substrate composed of the first five N-terminal amino acids of ghrelin.[40]

However, subsequent research indicated that ghrelin could be modified with acyl groups other than octanoate. In a study where rats were fed diets high in C6 or C10 fatty acids, the acylation state of ghrelin was observed to mirror the diet composition.[62] For example, consumption of high levels of C6 fatty acids led to detection of hexanoyl-ghrelin in the animal's bloodstream.[62] However, this *in vivo* study could not prove that GOAT was responsible for the alteration in ghrelin acylation. To investigate whether GOAT is capable of acylating ghrelin with fatty acids other than octanoate, Ohgusu and coworkers screened acyl donors with varying acyl chain lengths, including hexanoyl-CoA (C6, 6 carbons long), decanoyl-CoA (C10),

myristoyl-CoA (C14), and palmitoyl CoA (C16) for activity with the mouse form of GOAT.[41] They found that both hexanoyl-CoA and decanoyl-CoA showed activity as acyl donors, with GOAT exhibiting higher activity with hexanoyl-CoA than octanoyl-CoA. This suggests that cellular octanoyl-CoA levels are higher than hexanoyl-CoA to allow for ghrelin octanoylation.

Characterizing the range of acyl donors accepted by GOAT will aid in defining the size and nature of the acyl donor binding site within GOAT. Using the human isoform of GOAT (hGOAT) and a fluorescence-based GOAT peptide substrate developed in the Hougland lab, we have systematically investigated the activity of acyl-CoA donors in ghrelin acylation. These studies present the first step towards characterization of acyl donor selectivity by hGOAT.

Results and Discussion

Selection of acyl CoA donors for activity screening

To select acyl donors for screening, we started with the known octanoyl-CoA substrate for hGOAT and adjust the length of the acyl chain in two carbon increments to both longer and shorter acyl groups. Several groups, including our own, have shown that long chain acyl donors myristoyl CoA (C14) and palmitoyl-CoA (C16) do not serve as efficient cosubstrates for either the mouse or human forms of GOAT.[41] Based on this methodology and limiting criteria, we chose to screen five acyl donors for activity with hGOAT: acetyl-CoA (C2), butyryl-CoA (C4), hexanoyl-CoA (C6), decanoyl-CoA (C10), and lauroyl-CoA (C12).

Screening for ghrelin acylation activity using various acyl CoA's

Previous studies of hGOAT activity with octanoyl-CoA indicated that hGOAT activity reaches a maximum in the presence of 500 μM octanoyl-CoA.[46] For activity screening, we

investigated ghrelin acylation activity in the presence of either 500 μM or 1 mM of each acyl-donor. Following incubation of the GSSFLC$_{AcDan}$ peptide substrate with hGOAT and the acyl donors, reactions were analyzed using reverse-phase HPLC to detect the presence of the acylated GSSFLC$_{AcDan}$ peptide product.

Compared to control reactions lacking any acyl-CoA cosubstrate (green traces in Figure 18), new peaks corresponding to acylated forms of the GSSFLC$_{AcDan}$ substrate were observed in reactions with several of the acyl-CoA donors (Figure 18). In addition to the presence of the new peak with longer retention time indicating acylation of the GSSFLC$_{AcDan}$ substrate, the relation of the observed product reaction time to the length of the acyl-CoA donor acyl chain provides further evidence for ghrelin acylation. Under the reverse phase HPLC gradient used in this study, acylation of the GSSFLC$_{AcDan}$ peptide substrate with octanoyl-CoA leads to the formation of the octanoyl-GSSFLC$_{AcDan}$ product with a retention time of 12.1 minutes (Figure 18d), consistent with previous studies.[46] However, reaction with hexanoyl-CoA yields a new product peak with a retention time of 10 minutes and reaction with decanoyl-CoA produces an product peak with a retention time of ~14 min (Figures 18c and 18e). These results indicate that the human form of GOAT, like the mouse form studied by Ohgusu and coworkers,[41] can accept hexanoyl-CoA and decanoyl-CoA as acyl donors.
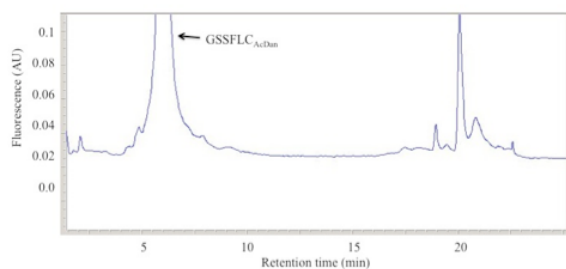
In addition to confirming similar acyl donor tolerances for the human and mouse forms of GOAT, the products from reaction with these three acyl donors establish a pattern relating the addition or subtraction of two methylene units from the acyl chain to an approximately two minute shift in product retention time under our HPLC conditions. This pattern predicts retention times for the acylated products of reaction with acetyl-CoA (6 minutes), butyryl-CoA (8 minutes), and lauroyl-CoA (16 minutes). Neither acetyl-CoA nor butyryl-CoA demonstrated

any evidence for acylation activity with hGOAT and GSSFLC$_{AcDan}$ at either 500 μM or 1 mM concentrations (Figures 18b, c, d, and e); it should be noted that the product peak for acylation by acetyl-CoA (if present) may be difficult to distinguish from the large peak for unreacted GSSFLC$_{AcDan}$ at 5-6 minutes retention time. However, reaction with lauroyl-CoA led to the formation of a new peak with a retention time of approximately 16 min, consistent with the predicted retention time for lauroyl- GSSFLC$_{AcDan}$ (Figure 18 l, and m).
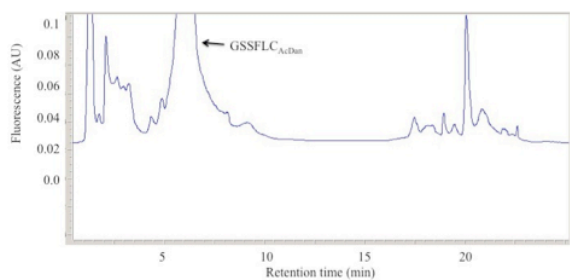
In reactions where a product peak was detected by HPLC, the area of the substrate and products peaks were integrated and the percent conversion was calculated (Figure 19). These integrations suggest that octanoyl-CoA serves as the best acyl donor for acylation of the GSSFLC$_{AcDan}$ substrate by hGOAT. The increase in percent conversion observed for hexanoyl-, decanoyl-, and lauroyl-CoA when the acyl-CoA concentration was increased from 500 mM to 1 mM suggests that these other acyl-CoA cosubstrates may not bind as tightly to hGOAT as octanoyl-CoA.

In summary, we have demonstrated that hGOAT can utilize a range of acyl-CoA cosubstrates to acylate ghrelin. This substrate promiscuity suggests that the acyl donor-binding pocket within hGOAT is flexible and can accommodate changes in acyl change lengths without loss of catalytic activity. This knowledge of the flexibility of the hGOAT binding pocket allows for inhibitor design of ghrelin acylation by hGOAT. Product-based inhibitors can be designed with various acyl length chains, ranging from six to twelve carbons.
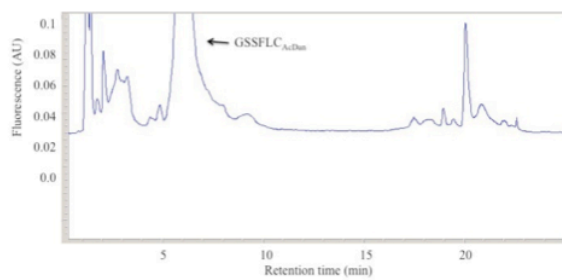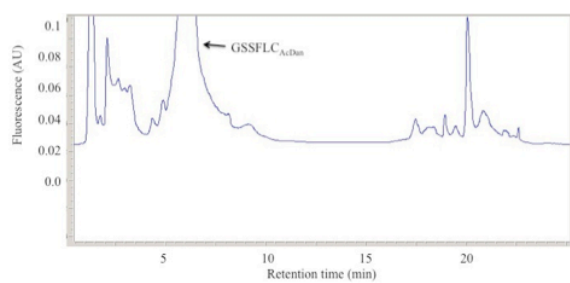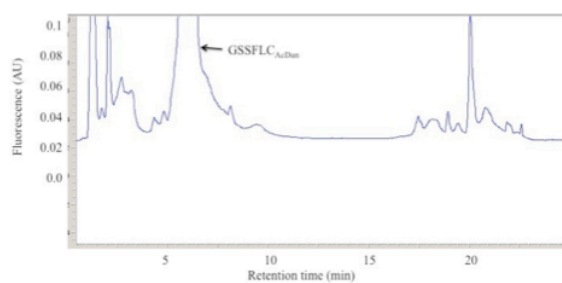
a.) control (no acyl-CoA)

b.) 500 μM acetyl-CoA

c.) 1000 μM acetyl-CoA

d.) 500 μM butyryl-CoA

e.) 1000 μM butyryl-CoA

f.) 500 μM hexanoyl-CoA

g.) 1000 μM hexanoyl-CoA

h.) 500 µM octanoyl-CoA

i.) 1000 µM octanoyl-CoA

j.) 500 µM decanoyl-CoA

k.) 1000 µM decanoyl-CoA

l.) 500 µM lauroyl-CoA
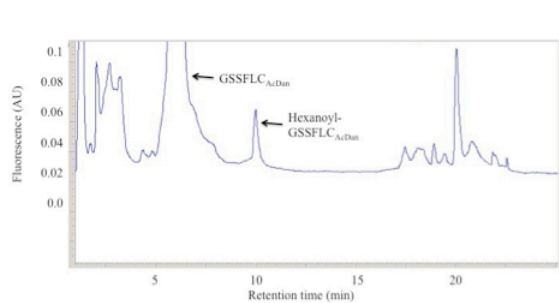
m.) 1000 µM lauroyl-CoA
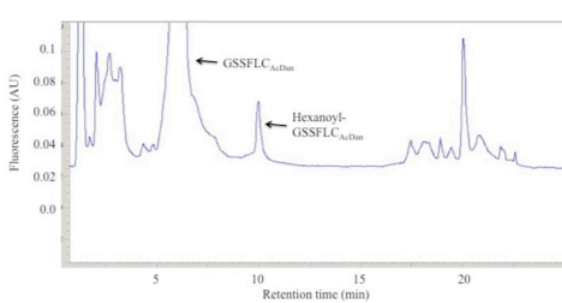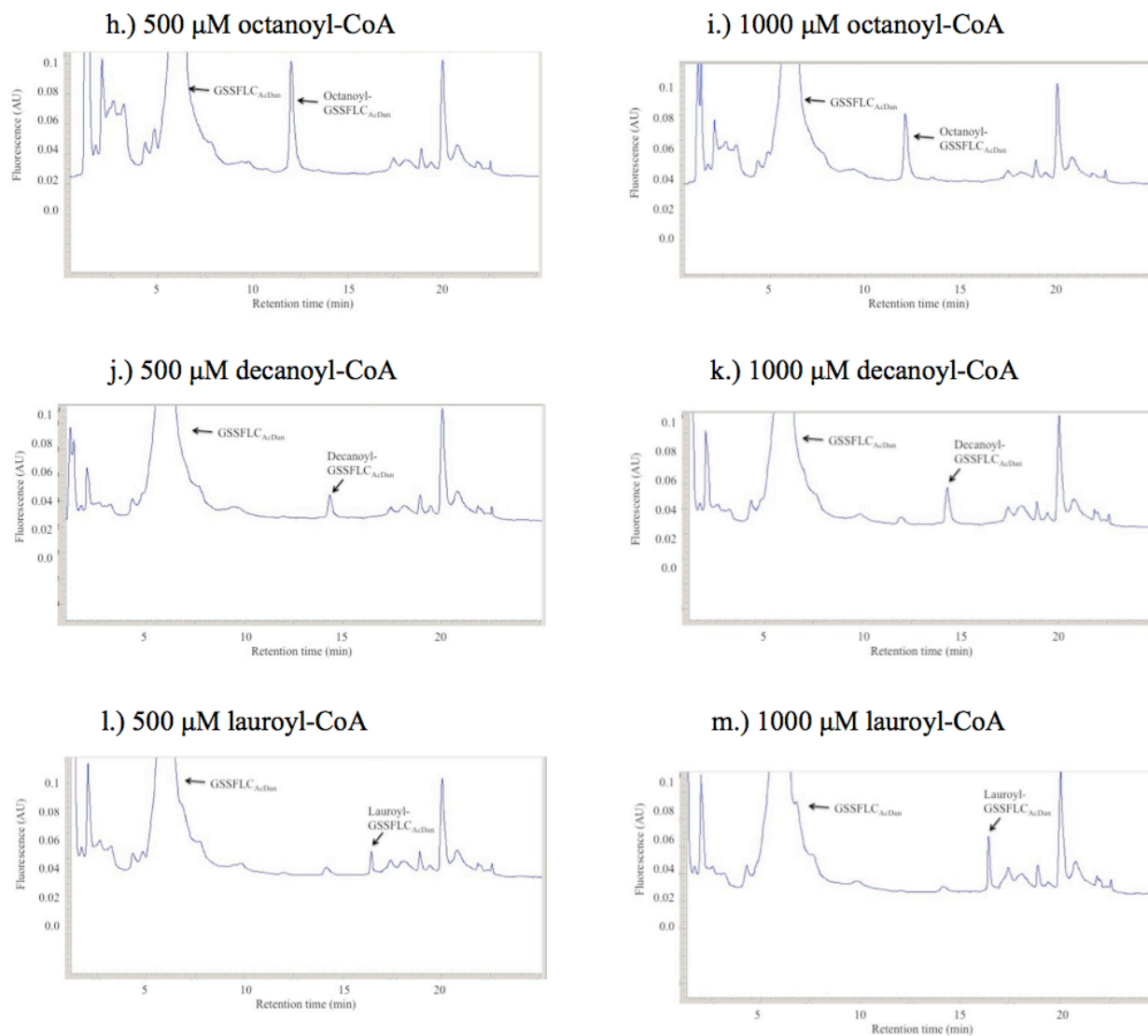
Figure 18. Screening of acyl-CoA reactivity with hGOAT. (a.) negative control (no acyl-CoA). (b. and c.) 500 µM and 1000 µM acetyl CoA; no evidence of acetylated product peak. (d. and e.) 500 µM and 1000 µM butyryl CoA; no evidence of butyrylated-peptide product peak. (f. and g.) 500 µM and 1000 µM hexanoyl CoA; potential hexanoyl-GSSFLC$_{AcDan}$ peak observed with a retention time of 10.0 minutes. (h. and i.) 500 µM and 1000 µM octanoyl CoA; octanoyl- GSSFLC$_{AcDan}$ observed with 12.1 minute retention time. (j. and k.) 500 µM and 1000 µM Decanoyl-CoA; potential decanoyl- GSSFLC$_{AcDan}$ detected with 14.4 minute retention time (l. and m.) 500 µM and 1000 µM lauroyl CoA; potential lauroyl-GSSFLC$_{AcDan}$ peak observed with retention time of 16.5 min.

Figure 19. Product peak areas for reaction with acyl-CoA donors with varying acyl chains lengths. Comparison of acyl-CoA activities is relative to the positive control octanoyl-CoA. Percent conversion was calculated integrating the areas of the peptide substrates and acylated peptide product peaks and dividing the area of the product peak by the total peptide area (substrate plus product).

Materials and Methods

General materials.

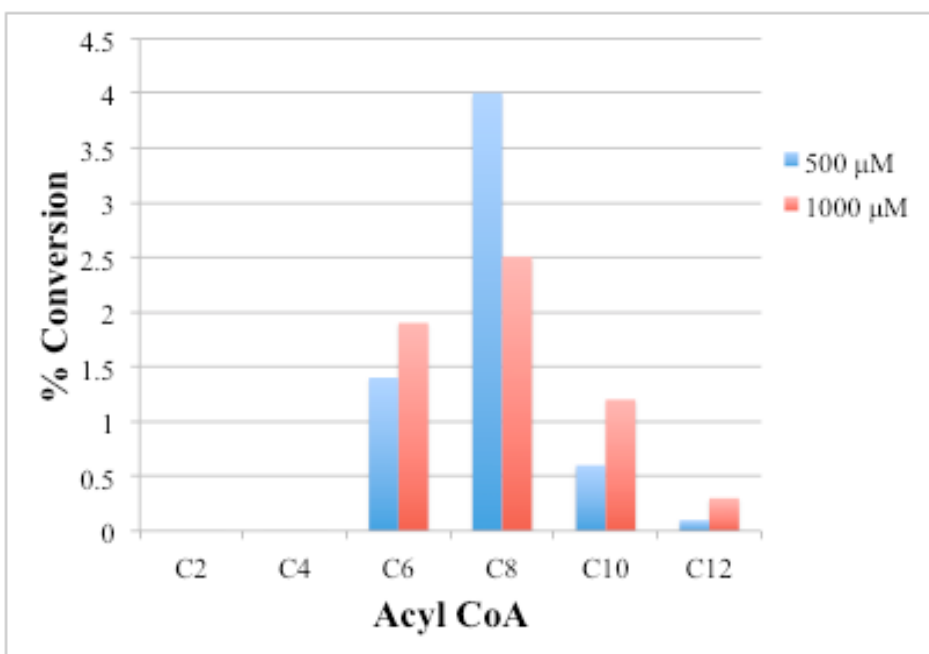Acetyl coenzyme A (acetyl CoA), butyryl CoA, hexanoyl CoA, octanoyl CoA, decanoyl CoA, and lauroyl CoA (Advent Bio) were solubilized in 10 mM Tris-HCl (pH 7.0) to 5 mM and stored at -80 °C until use (Darling).

hGOAT expression and purification

A gene encoding hGOAT with a His$_{10}$ tag at the C-terminus, an *EcoR*I restriction site at the 5' end and a *Xba*I restriction site at the 3' end was synthesized (Genscript). The gene hGOAT was cloned into the pFastBac Dual vector (Invitrogen) using the *EcoR*I and *Xba*I restriction sites. Baculovirus was then produced using the resulting pFastBac Dual-hGOAT vector and the Bac-to-Bac baculovirus expression system protocol (Invitrogen) following the manufacturer's instructions.

For protein expression, Sf9 insect cell cultures (1 x 10^6 cell/mL) were infected hGOAT baculovirus at a multiplicity of infection (MOI) of 10 and incubated at 27 °C with stirring (150 rpm) for 72 hours. Following protein expression, Sf9 cultures were harvested by centrifugation (500 x g, 5 minutes) at 4 °C. Cell pellets were resuspended in 1/20 culture volume of lysis buffer [150 mM NaCl, 50 mM Tris-HCl pH 7.0, 1 mM NaEDTA, 1 mM DTT, complete mini-tab protease inhibitor (Roche Pharmaceuticals), 10 µg/mL Pepstatin A, 100 µM bis (4-nitrophenyl) phosphate]. The resuspended cells were transferred to a dounce homogenizer and lysed by 40 dounce strokes on ice, followed by removal of cell debris by centrifugation (3000 x g, 5 minutes) at 4 °C. The membrane protein fraction was isolated from the resulting supernatant by ultracentrifugation (100,000 x g, 1 hour) at 4 °C. The isolated membrane fraction pellet was

resuspended in buffer (50 mM HEPES, pH 7.0) by pipetting (25 strokes). Protein concentration

was determined by Bradford assay (Bio-Rad, Hercules, CA), and the resuspended membrane

fractions were aliquoted (50 μL) and stored at -80 °C until use.

Acyl CoA activity assay

Membrane fractions from Sf9 cells expressing hGOAT variants were thawed on ice and

passed through an 18 gauge needle ten times. Membranes were then centrifuged (1000 x g, 1

min), with the supernatant collected and added to hGOAT reactions. Reactions contained the

desired concentration of membrane fraction as determined by Bradford assay (50 μg). Unless

noted otherwise, assays were performed with 1.5 μM acrylodanylated peptide substrate

(GSSFLC$_{AcDan}$), 500 μM acyl-CoA, and 50 mM HEPES pH 7.0 in a total volume of 50 mL.

Assays were initiated by addition of the acrylodanylated peptide substrate. Assays were

incubated at room temperature and stopped by addition of 50 μL of 20% acetic acid in

isopropanol. Assays were analyzed by reverse phase HPLC (Zorbax Eclipse XDB column, 4.6 x

150 mm) using a gradient from 30% acetonitrile in water containing 0.05% TFA to 63%

acetonitrile in water containing 0.05% TFA flowing at 1 mL/min over 14 min, followed by 100%

acetonitrile for 5 min; acrylodanylated peptides were detected by UV absorbance at 360 nm and

fluorescence (360 nm excitation, 485 nm emission). Peptide substrates typically eluted with a

retention time of 5-7 minutes, with the octanoylated peptide product eluting at ~12 min.

Chromatogram analysis and peak integration was performed using Chemstation for LC (Agilent

Technologies).

CHAPTER FOUR

CONCLUSIONS AND FUTURE DIRECTIONS

Investigating the active site of hGOAT in order to develop more potent inhibitors presents a promising avenue for treatment of various health conditions which may be tied to ghrelin signaling, such as type II diabetes, obesity, and Prader Willi Syndrome. Octanoylation of ghrelin by hGOAT provides an ideal target point for blocking ghrelin signaling. Specific and potent hGOAT inhibitors are needed to both validate ghrelin signaling as a therapeutic target and to serve as leads in preclinical trials. In order to develop potent novel hGOAT inhibitors, a greater understanding of the interactions within the ghrelin-hGOAT complex is required. Defining these interactions will be aided by identifying which regions/domains of hGOAT, and the specific residues within those regions, are most vital in ghrelin binding and catalysis.

To identify which domains and residues within hGOAT constitute the enzyme active site, we developed truncation mutants, loop mutants, and single point mutants of hGOAT to examine which regions within hGOAT are required for enzyme activity. When the truncation mutants that removed the first one, two, or three transmembrane domains and intervening soluble loops were tested for octanoylation activity, none exhibited activity in our *in vitro* assay using a short peptide mimic of ghrelin. This lack of activity may arise from disruption of the enzyme active site, overall enzyme destabilization, or insufficient protein expression. To test for disruption of the enzyme active site that could have occurred due to these mutations, we have generated

putative catalytic residue point mutations that will be tested for activity, which will tell us what residues need to be present in order for the enzyme to octanoylate ghrelin. To control for insufficient protein expression, we need to get a clean western blot using an antibody against GOAT.

Using the predicted transmembrane topology of hGOAT as a guide, we also attempted to express the predicted loop domains of hGOAT in attempt to generate a soluble form of hGOAT. Activity from these loop domain variants would both help identify the location of the enzyme active site and also provide a route to bacterial expression of hGOAT for use in enzyme purification and enzymological characterization. Unfortunately, the loop mutant constructs did not show any expression either by themselves or when fused to MBP or GST to increase protein solubility. Surprisingly, expression of neither MBP nor GST alone were detected when fused to the loop domain constructs, suggesting that attachment of the hGOAT loop domains to MBP or GST leads to severe protein destabilization. In an attempt to recover protein stability, the hGOAT loops are being cyclized with the use of split inteins. Inteins are segments of protein that excise themselves from nascent polypeptide chains following translation, and a resulting peptide bond is formed between the remaining portions.[63] Using these split inteins for the hGOAT loop expressions in *E. coli* should hopefully help in stabilization of the native structure of the loops, which has been shown to be effective in previous studies when proteins were cyclized by peptide-bond formation of the NH_2- and COOH- terminal ends.[64, 65, 66] In addition to offering protein stability, these split inteins are also useful in protection from exo-proteases, which cleave at the terminal ends of proteins.[67]

Development of single point mutants was then done with the idea that single point mutants would provide less perturbation of the enzyme rather than excising whole domains in

order to identify which residues are required for activity, which could provide vital mechanistic information. The residues chosen for mutagenesis were selected based upon two criteria: amino acid conservation across the known MBOAT4 isoforms and the potential to lie in loop domains rather than transmembrane helices, as predicted by the TMHMM server. We also limited our selections to residues that could bind and position a catalytic metal ion or participate in general acid-base catalysis. Of particular interest are residues His258, Asp262, and Asp263, located in loop D, which form a sequence consistent with the Hx_4D catalytic motif observed in glycerol phosphate acyltransferases (GPATs). In GPATs, these residues have been shown to participate in catalysis by forming a "catalytic triad" similar to those seen in serine proteases using the conserved histidine and aspartate residues along with a hydroxyl group from the substrate to be acylated.[50, 53, 54] The similarity of the "HWILDD" motif in hGOAT to the HX_4D motif from GPATs may indicate the potential for a shared catalytic mechanism and suggests that hGOAT may employ and active site histidine as a general base when catalyzing ghrelin acylations. If the His258, Asp262, or Asp263 mutants were to result in a loss of activity, it may be evidence that these are putative catalytic residues potentially located in the hGOAT active site. Vital mechanistic information on hGOAT can be acquired if any of these mutants results in a loss of a hGOAT activity. Additionally, it has recently been found that hGOAT also octanoylates a cysteine residue as well a serine (Joe Darling, unpublished data). Taking into consideration that the thiol group of cysteine would be a far better nucleophile than the hydroxyl group of serine, if one of these mutants were to lose activity with the wild type substrate ($GSSFLC_{AcDan}$) due to disruption of the "catalytic triad" machinery, the Cys3 substrate ($GSCFLC_{AcDan}$) theoretically should not experience the same drop in activity due to its ability to be a better nucleophile and not require the general His base to abstract its proton. This trend would give further insight as to

75

how putative catalytic residues interact with one another in the hGOAT active site and therefore help in developing hGOAT inhibitors.

To complement our studies using enzyme modification to locate the hGOAT active site, we also examined the range of acyl-CoA donors accepted by hGOAT to ascertain the flexibility of the acyl donor binding pocket within the hGOAT active site. Similar studies of the mouse isoform of GOAT indicated some promiscuity in the activity of the acyl-CoA donor.[41] We tested a set of five acyl-CoA donors with varied acyl chain lengths- acetyl-CoA (C2 acyl chain), butyryl-CoA (C4), hexanoyl-CoA (C6), decanoyl-CoA (C10), and lauroyl-CoA (C12). We found that although octanoyl-CoA provided the best octanoylation efficiency of the GSSFLC$_{AcDan}$ substrate in our HPLC assay, hexanoyl-CoA, decanoyl-CoA, and lauroyl-CoA demonstrate hGOAT-catalyzed acylation activity as well, indicating that the acyl binding site within hGOAT accepts a range of acyl chain lengths. The increased substrate acylation observed with hexanoyl-CoA, decanoyl-CoA, and lauroyl-CoA at a higher acyl-CoA concentration (1 mM versus 500 μM) suggests that these acyl-CoA donors may not bind as tightly to hGOAT as octanoyl-CoA. Therefore, hGOAT has been shown to utilize a range of acyl-CoA cosubstrates to acylate ghrelin, suggesting that the acyl-donor binding pocket within hGOAT can accommodate changes in acyl chain lengths without loss of catalytic activity. Using this information, optimization of the acyl chain length can be explored to maximize inhibitor binding. In addition, the alternative acylated forms of ghrelin can be further investigated for their biological impact to see if they bind differently to the GHSr1a receptor or to other receptors.

In addition to the work described herein aimed at identifying regions of hGOAT required for activity, substrate photocrosslinking will be used to identify the amino acids within hGOAT potentially involved in ghrelin binding and acylation. Photocrosslinking involves incorporation

of a photoreactive probe into a target molecule such as an enzyme substrate. Following the target substrate binding to the enzyme, the photoreactive probe is activated by irradiation with UV light to generate a covalent bond between the enzyme and the substrate.[68, 69, 70] By locating the resulting covalent crosslinks within the enzyme primary sequence using mass spectrometry, we will identify amino acids within hGOAT that are spatially close to the target substrate bearing the photocrosslinking group. A well-known photocrosslinker used as a probe in studying protein-protein interaction is benzophenone, which is activated by UV irradiation between 350-365 nm.[68, 71] This photoactivation leads to formation of a transient diradical that can subsequently react with methionine sidechains and C-H bonds.[68, 71] Due to the persistence of the activated diradical with a lifetime of 120 μs and the ability of benzophenone to be repeatedly illuminated and activated in the event of diradical recombination, benzophenone has a high crosslinking efficiency.[68, 71] In 2010, Barnett and coworkers were successfully able to covalently crosslink their GO-CoA-Tat inhibitor to solubilized and microsomal GOAT by replacing either Phe4 or Leu5 of their inhibitor with photoreactive amino acid benzoyl-phenylalanine, giving proof that the inhibitor was indeed binding to GOAT.[42] Additional photo labeling work has also been done on a different membrane protein, Ras converting enzyme (Rce1p), to find residues in or near the active site. For this particular enzyme, a benzophenone containing peptide substrate analogue was employed, and shown to be a substrate for Rce1p.[72, 73] When structural models are not available (as is the generally the case with membrane bound proteins), substrate photocrosslinking has shown to be an efficient way to identify regions near the active site for subsequent study, such as where to perform additional site directed mutagenesis.

The overall goal of my project has been to understand the enzyme selectivity and catalytic mechanism of hGOAT. Defining how hGOAT binds ghrelin and catalyzes its

octanoylation using the single-point mutations and photo-crosslinking, more potent and novel hGOAT inhibitors can be developed. By generating various hGOAT mutants constructs, we are well on our way towards testing these constructs for hGOAT octanoylation of ghrelin, which will further our understanding on which regions of hGOAT are critical in catalysis so that more potent inhibitors can be developed. Inhibiting GOAT provides a direct pathway to modulate ghrelin-dependent signaling proposed to be involved in diseases such as Prader Willi syndrome, type II diabetes, and obesity arising from aberrant levels of ghrelin, and could be used for therapeutic treatment.

REFERENCES

(1)   Kojima, M.; Hosoda, H.; Date, Y.; Nakazato, M.; Matsuo, H.; Kangawa, K. *Nature* **1999**, *402*, 656–660.

(2)   Korbonits, M.; Ciccarelli, E.; Ghigo, E.; Grossman, A. B. *Growth Horm. Igf Res.* **1999**, *9*, 93–99.

(3)   Taylor, M. S.; Hwang, Y.; Hsiao, P.-Y.; Boeke, J. D.; Cole, P. A. *Methods Enzymol.* **2012**, *514*, 205–228.

(4)   Wierup, N.; Svensson, H.; Mulder, H.; Sundler, F. *Regul. Pept.* **2002**, *107*, 63–69.

(5)   Date, Y.; Kojima, M.; Hosoda, H.; Sawaguchi, A.; Mondal, M. S.; Suganuma, T.; Matsukura, S.; Kangawa, K.; Nakazato, M. *Endocrinology* **2000**, *141*, 4255–4261.

(6)   Broglio, F.; Arvat, E.; Benso, A.; Gottero, C.; Muccioli, G.; Papotti, M.; van der Lely, A. J.; Deghenghi, R.; Ghigo, E. *J. Clin. Endocrinol. Metab.* **2001**, *86*, 5083–5086.

(7)   Van der Lely, A. J.; Tschöp, M.; Heiman, M. L.; Ghigo, E. *Endocr. Rev.* **2004**, *25*, 426–457.

(8)   Romero, A.; Kirchner, H.; Heppner, K.; Pfluger, P. T.; Tschöp, M. H.; Nogueiras, R. *Eur. J. Endocrinol. Eur. Fed. Endocr. Soc.* **2010**, *163*, 1–8.

(9)   Toshinai, K.; Mondal, M. S.; Nakazato, M.; Date, Y.; Murakami, N.; Kojima, M.; Kangawa, K.; Matsukura, S. *Biochem. Biophys. Res. Commun.* **2001**, *281*, 1220–1225.

(10)   Tschöp, M.; Weyer, C.; Tataranni, P. A.; Devanarayan, V.; Ravussin, E.; Heiman, M. L. *Diabetes* **2001**, *50*, 707–709.

(11)   Cummings, D. E.; Overduin, J. *J. Clin. Invest.* **2007**, *117*, 13–23.

(12)   Cummings, D. E.; Purnell, J. Q.; Frayo, R. S.; Schmidova, K.; Wisse, B. E.; Weigle, D. S. *Diabetes* **2001**, *50*, 1714–1719.

(13)   Otto, B.; Cuntz, U.; Fruehauf, E.; Wawarta, R.; Folwaczny, C.; Riepl, R. L.; Heiman, M. L.; Lehnert, P.; Fichter, M.; Tschöp, M. *Eur. J. Endocrinol. Eur. Fed. Endocr. Soc.* **2001**, *145*, 669–673.

(14)   Tanaka, M.; Naruo, T.; Yasuhara, D.; Tatebe, Y.; Nagai, N.; Shiiya, T.; Nakazato, M.; Matsukura, S.; Nozoe, S. *Psychoneuroendocrinology* **2003**, *28*, 829–835.

(15)   Ariyasu, H.; Takaya, K.; Tagami, T.; Ogawa, Y.; Hosoda, K.; Akamizu, T.; Suda, M.; Koh, T.; Natsui, K.; Toyooka, S.; Shirakami, G.; Usui, T.; Shimatsu, A.; Doi, K.; Hosoda, H.; Kojima, M.; Kangawa, K.; Nakao, K. *J. Clin. Endocrinol. Metab.* **2001**, *86*, 4753–4758.

(16)   Hinney, A.; Hoch, A.; Geller, F.; Schäfer, H.; Siegfried, W.; Goldschmidt, H.; Remschmidt, H.; Hebebrand, J. *J. Clin. Endocrinol. Metab.* **2002**, *87*, 2716.

(17)   Wang, H.-J.; Geller, F.; Dempfle, A.; Schäuble, N.; Friedel, S.; Lichtner, P.; Fontenla-Horro, F.; Wudy, S.; Hagemann, S.; Gortner, L.; Huse, K.; Remschmidt, H.; Bettecken, T.; Meitinger, T.; Schäfer, H.; Hebebrand, J.; Hinney, A. *J. Clin. Endocrinol. Metab.* **2004**, *89*, 157–162.

(18)   Korbonits, M.; Gueorguiev, M.; O'Grady, E.; Lecoeur, C.; Swan, D. C.; Mein, C. A.; Weill, J.; Grossman, A. B.; Froguel, P. *J. Clin. Endocrinol. Metab.* **2002**, *87*, 4005–4008.

(19)   Cummings, D. E.; Clement, K.; Purnell, J. Q.; Vaisse, C.; Foster, K. E.; Frayo, R. S.; Schwartz, M. W.; Basdevant, A.; Weigle, D. S. *Nat. Med.* **2002**, *8*, 643–644.

(20)   Lim, C. T.; Kola, B.; Korbonits, M. *Rev. Endocr. Metab. Disord.* **2011**, *12*, 173–186.

(21) Wierup, N.; Yang, S.; McEvilly, R. J.; Mulder, H.; Sundler, F. *J. Histochem. Cytochem. Off. J. Histochem. Soc.* **2004**, *52*, 301–310.

(22) Dezaki, K.; Yada, T. *Methods Enzymol.* **2012**, *514*, 317–331.

(23) Reimer, M. K.; Pacini, G.; Ahrén, B. *Endocrinology* **2003**, *144*, 916–921.

(24) Dezaki, K.; Hosoda, H.; Kakei, M.; Hashiguchi, S.; Watanabe, M.; Kangawa, K.; Yada, T. *Diabetes* **2004**, *53*, 3142–3151.

(25) Cui, C.; Ohnuma, H.; Daimon, M.; Susa, S.; Yamaguchi, H.; Kameda, W.; Jimbu, Y.; Oizumi, T.; Kato, T. *Peptides* **2008**, *29*, 1241–1246.

(26) Qader, S. S.; Håkanson, R.; Rehfeld, J. F.; Lundquist, I.; Salehi, A. *Regul. Pept.* **2008**, *146*, 230–237.

(27) Heppner, K. M.; Tong, J.; Kirchner, H.; Nass, R.; Tschöp, M. H. *Curr. Opin. Endocrinol. Diabetes Obes.* **2011**, *18*, 50–55.

(28) Delhanty, P. J. D.; van der Lely, A. J. *Peptides* **2011**, *32*, 2309–2318.

(29) Zhou, A.; Webb, G.; Zhu, X.; Steiner, D. F. *J. Biol. Chem.* **1999**, *274*, 20745–20748.

(30) Zhu, X.; Cao, Y.; Voogd, K.; Voodg, K.; Steiner, D. F. *J. Biol. Chem.* **2006**, *281*, 38867–38870.

(31) Kojima, M.; Kangawa, K. *Physiol. Rev.* **2005**, *85*, 495–522.

(32) Takahashi, T.; Ida, T.; Sato, T.; Nakashima, Y.; Nakamura, Y.; Tsuji, A.; Kojima, M. *J. Biochem. (Tokyo)* **2009**.

(33) Yang, J.; Brown, M. S.; Liang, G.; Grishin, N. V.; Goldstein, J. L. *Cell* **2008**, *132*, 387–396.

(34) Gutierrez, J. A.; Solenberg, P. J.; Perkins, D. R.; Willency, J. A.; Knierman, M. D.; Jin, Z.; Witcher, D. R.; Luo, S.; Onyia, J. E.; Hale, J. E. *Proc. Natl. Acad. Sci. U. S. A.* **2008**, *105*, 6320–6325.

(35) Buglino, J. A.; Resh, M. D. *J. Biol. Chem.* **2008**, *283*, 22076–22088.

(36) Chamoun, Z.; Mann, R. K.; Nellen, D.; von Kessler, D. P.; Bellotto, M.; Beachy, P. A.; Basler, K. *Science* **2001**, *293*, 2080–2084.

(37) Hofmann, K. *Trends Biochem. Sci.* **2000**, *25*, 111–112.

(38) Kadowaki, T.; Wilder, E.; Klingensmith, J.; Zachary, K.; Perrimon, N. *Genes Dev.* **1996**, *10*, 3116–3128.

(39) Takada, R.; Satomi, Y.; Kurata, T.; Ueno, N.; Norioka, S.; Kondoh, H.; Takao, T.; Takada, S. *Dev. Cell* **2006**, *11*, 791–801.

(40) Yang, J.; Zhao, T.-J.; Goldstein, J. L.; Brown, M. S. *Proc. Natl. Acad. Sci. U. S. A.* **2008**, *105*, 10750–10755.

(41) Ohgusu, H.; Shirouzu, K.; Nakamura, Y.; Nakashima, Y.; Ida, T.; Sato, T.; Kojima, M. *Biochem. Biophys. Res. Commun.* **2009**, *386*, 153–158.

(42) Barnett, B. P.; Hwang, Y.; Taylor, M. S.; Kirchner, H.; Pfluger, P. T.; Bernard, V.; Lin, Y.; Bowers, E. M.; Mukherjee, C.; Song, W.-J.; Longo, P. A.; Leahy, D. J.; Hussain, M. A.; Tschöp, M. H.; Boeke, J. D.; Cole, P. A. *Science* **2010**, *330*, 1689–1692.

(43) Teubner, B. J. W.; Garretson, J. T.; Hwang, Y.; Cole, P. A.; Bartness, T. J. *Horm. Behav.* **2013**, *63*, 667–673.

(44) Garner, A. L.; Janda, K. D. *Angew. Chem. Int. Ed Engl.* **2010**, *49*, 9630–9634.

(45) Garner, A. L.; Janda, K. D. *Chem. Commun. Camb. Engl.* **2011**, *47*, 7512–7514.

(46) Darling, J. E.; Prybolsky, E. P.; Sieburg, M.; Hougland, J. L. *Anal. Biochem.* **2013**, *437*, 68–76.

(47) A. Krogh, B. Larsson, G. von Heijne, and E. L. L. Sonnhammer._Predicting transmembrane protein topology with a hidden Markov model: Application to complete genomes._Journal of Molecular Biology, 305(3):567-580, January 2001.

(48) Hernick, M.; Fierke, C. A. *Arch. Biochem. Biophys.* **2005**, *433*, 71–84.

(49) Cole, K. E.; Gattis, S. G.; Angell, H. D.; Fierke, C. A.; Christianson, D. W. *Biochemistry (Mosc.)* **2011**, *50*, 258–265.

(50) Zhang, Y.-M.; Rock, C. O. *J. Lipid Res.* **2008**, *49*, 1867–1874.

(51) Lightner, V. A.; Larson, T. J.; Tailleur, P.; Kantor, G. D.; Raetz, C. R.; Bell, R. M.; Modrich, P. *J. Biol. Chem.* **1980**, *255*, 9413–9420.

(52) Green, P. R.; Merrill, A. H., Jr; Bell, R. M. *J. Biol. Chem.* **1981**, *256*, 11151–11159.

(53) Heath, R. J.; Rock, C. O. *J. Bacteriol.* **1998**, *180*, 1425–1430.

(54) Lewin, T. M.; Wang, P.; Coleman, R. A. *Biochemistry (Mosc.)* **1999**, *38*, 5764–5771.

(55) Walter, P.; Johnson, A. E. *Annu. Rev. Cell Biol.* **1994**, *10*, 87–119.

(56) Baculovirus Expression System with Gateway® Technology - DNA Vectors http://www.invitrogen.com/1/1/12651-baculovirus-expression-system-gateway-technology.html (accessed May 19, 2013).

(57) Mims, M. P.; Sturgis, C. B.; Sparrow, J. T.; Morrisett, J. D. *Biochemistry (Mosc.)* **1993**, *32*, 9215–9220.

(58) Prendergast, F. G.; Meyer, M.; Carlson, G. L.; Iida, S.; Potter, J. D. *J. Biol. Chem.* **1983**, *258*, 7541–7544.

(59) Fox, J. D.; Waugh, D. S. *Methods Mol. Biol. Clifton Nj* **2003**, *205*, 99–117.

(60) Studier, F. W. *Protein Expr. Purif.* **2005**, *41*, 207–234.

(61) Wagner, S.; Klepsch, M. M.; Schlegel, S.; Appel, A.; Draheim, R.; Tarry, M.; Högbom, M.; van Wijk, K. J.; Slotboom, D. J.; Persson, J. O.; de Gier, J.-W. *Proc. Natl. Acad. Sci. U. S. A.* **2008**, *105*, 14371–14376.

(62) Nishi, Y.; Mifune, H.; Kojima, M. *Methods Enzymol.* **2012**, *514*, 303–315.

(63) Paulus, H. *Annu. Rev. Biochem.* **2000**, *69*, 447–496.

(64) Iwai, H.; Plückthun, A. *Febs Lett.* **1999**, *459*, 166–172.

(65) Iwai, H.; Lingel, A.; Pluckthun, A. *J. Biol. Chem.* **2001**, *276*, 16548–16554.

(66) Scott, C. P.; Abel-Santos, E.; Wall, M.; Wahnon, D. C.; Benkovic, S. J. *Proc. Natl. Acad. Sci. U. S. A.* **1999**, *96*, 13638–13643.

(67) Williams, N. K.; Prosselkov, P.; Liepinsh, E.; Line, I.; Sharipo, A.; Littler, D. R.; Curmi, P. M. G.; Otting, G.; Dixon, N. E. *J. Biol. Chem.* **2002**, *277*, 7790–7798.

(68) Tanaka, Y.; Bond, M. R.; Kohler, J. J. *Mol. Biosyst.* **2008**, *4*, 473–480.

(69) SINGH, A.; THORNTON, E. R.; WESTHEIMER, F. H. *J. Biol. Chem.* **1962**, *237*, 3006–3008.

(70) Brunner, J. *Annu. Rev. Biochem.* **1993**, *62*, 483–514.

(71) Dormán, G.; Prestwich, G. D. *Biochemistry (Mosc.)* **1994**, *33*, 5661–5673.

(72) Kyro, K.; Manandhar, S. P.; Mullen, D.; Schmidt, W. K.; Distefano, M. D. *Bioorg. Med. Chem.* **2010**, *18*, 5675–5684.

(73) Kyro, K.; Manandhar, S. P.; Mullen, D.; Schmidt, W. K.; Distefano, M. D. *Bioorg. Med. Chem.* **2011**, *19*, 7559–7569.

VITA

Rosemary Loftus was born in Portsmouth, Virginia. After graduating from Paul VI Catholic High School in Fairfax, VA in 2007, she went on to attend Christopher Newport University in Newport News, VA. She graduated from there with a Bachelor's of Science Degree in Chemistry in 2011. In August of 2011, she moved to Syracuse, New York to pursue her Master's of Science in Chemistry at Syracuse University.

Permanent address: 411 Kings Park Drive Extension Apt D

Liverpool, NY 13090